

Supplementary Information for

Deep Eutectic Solvents on a Tightrope: Balancing the Entropy and Enthalpy of Mixing

Adriaan van den Bruinhorst^{1,*}, Chiara Corsini¹, Guillaume Depraetère¹,
Nithavong Cam¹, Agílio Pádua¹, and Margarida Costa Gomes^{1,*}

¹École Normale Supérieure de Lyon and CNRS, Laboratoire de Chimie, Ionic
Liquids Group, 46 allée d'Italie, 69364, Lyon Cedex 7, France

*Corresponding authors: margarida.costa-gomes@ens-lyon.fr,
adriaan.van-den-bruinhorst@ens-lyon.fr

March 11, 2024

Contents

SI-1 Supplementary Methods	S2
SI-1.1 Materials	S2
SI-1.2 Karl-Fischer titration	S2
SI-1.3 Fitting the heat of mixing	S2
SI-1.4 Differential scanning calorimetry	S3
SI-1.5 Molecular dynamics simulations	S4
SI-2 Supplementary Discussion	S7
SI-2.1 Impact of heat capacity change on excess properties	S7
SI-3 Supplementary Figures	S11
SI-4 Supplementary Tables	S19

SI–1 Supplementary Methods

SI–1.1 Materials

Table S1 Overview of compounds used in this study as well as their abbreviations, CAS number, source, and purity

Compound	Abbreviation	CAS	Supplier	Purity ^a (%)
choline chloride	ChCl	67-48-1	Acros Chemicals	99
water	H ₂ O	7732-18-5	Sigma-Aldrich	n.r. ^b
ethylene glycol	EG	107-21-1	Sigma-Aldrich	>99.5
1,3-propanediol	13PD	504-63-2	Alfa Aesar	99

^a As reported by supplier

^b HPLC plus grade

SI–1.2 Karl-Fischer titration

Water contents were determined by Karl-Fischer titration using a Mettler-Toledo C20S coulometer coupled to an analytical balance (0.01 mg resolution) and with Hydralan coulomat E as medium. Liquids were injected through the septum using a needled syringe, and solid ChCl was added using a tailor-made solids syringe adapted to the coulometer glass cell that can be sealed under a dry atmosphere. Additions contained at least 100 µg of water, and reported values are the average of at least three additions. (Add picture of dosing unit)

SI–1.3 Fitting the heat of mixing

The heat effect of mixing (Q) as measured from calorimetry can be related to the partial molar excess enthalpy (H_i^E) of each of the constituents:

$$Q = \Delta n_1 (H_1^E(x_{2,\text{fin}}^{\text{cell}}) - H_1^E(x_2^{\text{syr}})) + \\ \Delta n_2 (H_2^E(x_{2,\text{fin}}^{\text{cell}}) - H_2^E(x_2^{\text{syr}})) + \\ n_1^{\text{cell}} (H_1^E(x_{2,\text{fin}}^{\text{cell}}) - H_1^E(x_{2,\text{ini}}^{\text{cell}})) + \\ n_2^{\text{cell}} (H_2^E(x_{2,\text{fin}}^{\text{cell}}) - H_2^E(x_{2,\text{ini}}^{\text{cell}})) \quad (\text{S1})$$

where n_i are the moles of i , Δn_i the added moles of i , and x_i the mole fraction of i . Superscripts "cell" and "syr" refer to the sample cell and the syringe, respectively. Subscripts "ini" and "fin" refer to before and after the injection, respectively. The pure liquids are taken as component 1 and ChCl as component 2. For small injections made with pure liquids, $\Delta n_2 = H_{\text{m},1}^E(x_2^{\text{syr}}) = 0$. As a consequence, the last two terms of Eq. S1 are negligible as compared to the first and H_1^E can be estimated from the peak integrals directly:

$$\frac{Q}{\Delta n_1} \approx H_1^E(x_{2,\text{fin}}^{\text{cell}}). \quad (\text{S2})$$

To integrate this data and obtain the total enthalpy of mixing H^E , we fitted H_1^E from ITC and H_2^E from dissolution calorimetry to a Redlich-Kister polynomial. However, we also made injections with ChCl solutions. In these cases, all H_i^E are significant and Eq. S2 does not hold. These data can still be accounted for by describing each H_i^E/RT with a Redlich-Kister

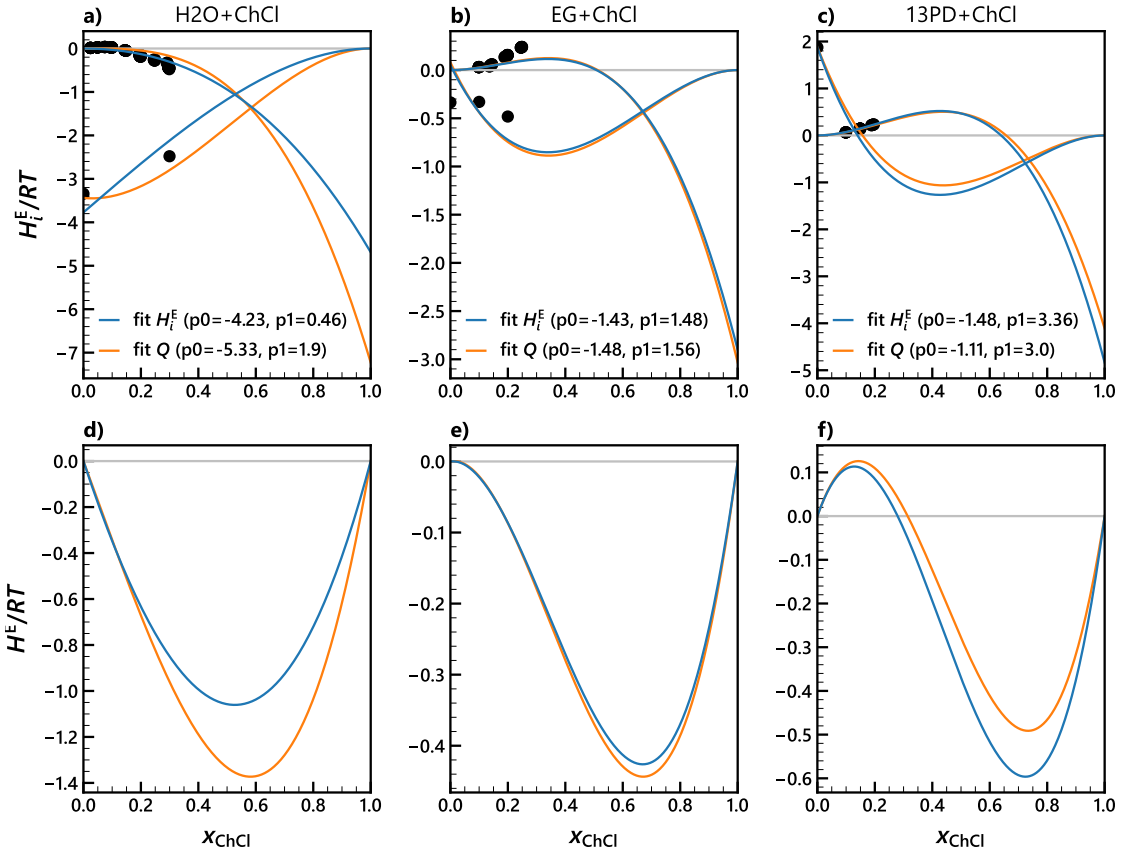


Fig. S1 Normalised partial molar excess enthalpy (H_i^E) data for **a)** water (H_2O) + choline chloride (ChCl), **b)** ethylene glycol (EG) + ChCl, and **c)** 1,3-propanediol (13PD) + ChCl. Values were fit directly to H_i^E/RT (blue) or to $Q_{\text{inj}}/RT \sum \Delta n_i$ (orange) using a first-order Redlich–Kister polynomial.

The

polynomial and fitting $Q_{\text{inj}}/RT \sum \Delta n_i$. We normalised with the total injected moles to avoid larger injections weighing stronger in the objective function. We also normalised with RT to obtain the parameters for the normalised excess properties directly. Fig. S1 shows the difference between fitting H_i^E/RT data only or $Q_{\text{inj}}/RT \sum \Delta n_i$. We opted for fitting $Q_{\text{inj}}/RT \sum \Delta n_i$, despite the slight underrepresentation of H_i^E . By fitting $Q_{\text{inj}}/RT \sum \Delta n_i$ we include all measured data points (see Tables S10–S12) and thus the most thermodynamic information.

SI-1.4 Differential scanning calorimetry

We observed strong supercooling behaviour for EG + ChCl and 13PD + ChCl, not showing any crystallisation peak upon a regular cooling–heating scan. We could overcome this by performing various heating/cooling cycles between the glass transition temperature and the melting point. The temperature program that allowed us to crystallise the sample is described below:

1. Heat from 30 °C to 60 °C at 10 °C/min
2. Hold 1 h at 60 °C
3. Cool from 60 °C to -80 °C at 10 °C/min
4. Hold 1 min at -80 °C
5. Heat from -80 °C to -30 °C at 1 °C/min
6. Hold 1 min at -30 °C
7. Cool from -30 °C to -80 °C at 1 °C/min
8. Hold 1 min at -80 °C
9. Heat from -80 °C to -35 °C at 1 °C/min
10. Hold 1 h at -35 °C
11. Cool from -35 °C to -60 °C at 10 °C/min
12. Hold 1 min at -60 °C

At the end of this cycle, sample is crystallised and the acquisition run is performed at a heating rate of 1, 2, 5 or 10 °C/min. A typical thermogram of this acquisition run is shown in figure S2.

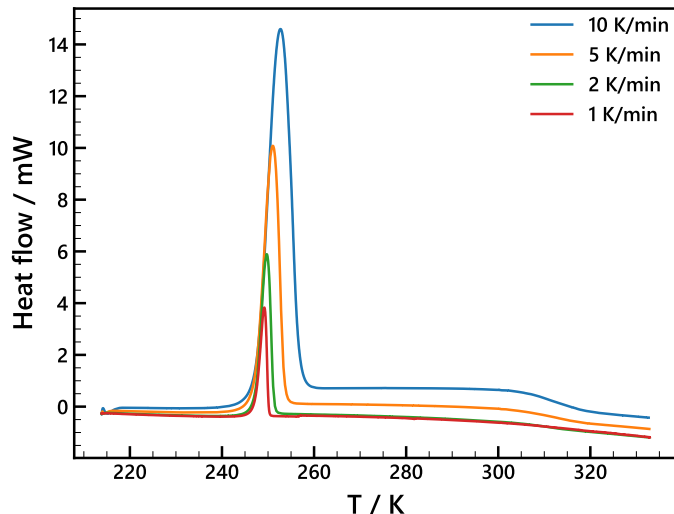


Fig. S2 Representative DSC thermogram upon heating EG + ChCl ($x_{\text{ChCl}} = 0.35$) at various heating rates. Endotherms up.

SI-1.5 Molecular dynamics simulations

The expected coordination number taking into account the change in ChCl concentration from x_{ChCl}^0 to x_{ChCl}^1 was calculated by

$$n_{\text{coord}}^{\text{exp}}(x_{\text{ChCl}}^1) = n_{\text{coord}}(x_{\text{ChCl}}^0) \frac{n_{\text{acc}}(x_{\text{ChCl}}^1)n_{\text{tot}}(x_{\text{ChCl}}^0)}{n_{\text{acc}}(x_{\text{ChCl}}^0)n_{\text{tot}}(x_{\text{ChCl}}^1)} \quad (\text{S3})$$

where n_{coord} , n_{acc} and n_{tot} are the coordination number, the number of acceptor atoms and the total number of atoms in the system, respectively.

Table S2 Composition of the simulated systems

x_{ChCl}	Number of ChCl	Number of HBD	Total number of atoms
Ethylene glycol			
0.0	0	1500	15000
0.1	135	1215	15120
0.3	336	784	15232
Water			
0.0	0	5000	15000
0.1	309	2781	15141
0.3	522	1218	15138

Table S3 Calculated liquid densities compared with experimental data.

$\rho(T_0)/\text{g}\cdot\text{cm}^{-3}$	Simulation	Experiment
x_{ChCl}		
Ethylene glycol	$T_0 = 333 \text{ K}$	
0.0	1.070 ± 0.004	1.08398^\dagger
0.1	1.054 ± 0.004	$1.090 \pm 0.002^*$
0.3	1.054 ± 0.004	$1.097 \pm 0.002^*$
Water	$T_0 = 353 \text{ K}$	
0.0	0.955 ± 0.004	0.97179^\ddagger
0.1	1.096 ± 0.003	$1.029 \pm 0.002^*$
0.3	1.140 ± 0.003	$1.073 \pm 0.002^*$

* See Fig. S3 and S4; \dagger From^[1]; \ddagger From^[2].

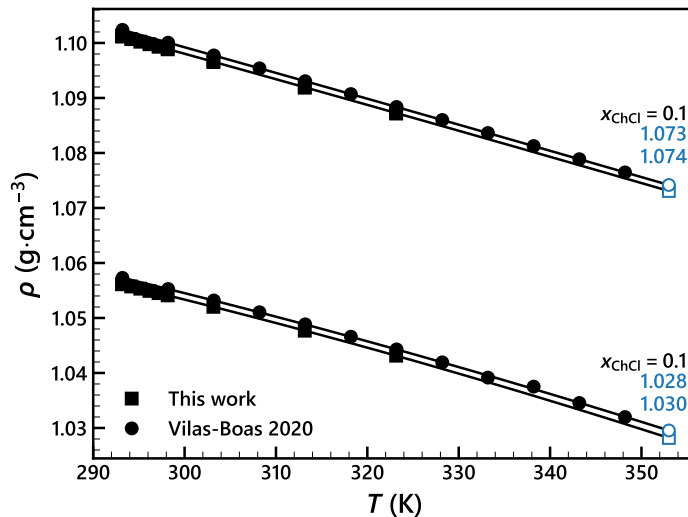


Fig. S3 Estimated densities for $\text{H}_2\text{O} + \text{choline chloride} (\text{ChCl})$ at mole fractions $x_{\text{ChCl}} = 0.1$ and $x_{\text{ChCl}} = 0.3$ by extrapolating the data to 353 K using a second-order polynomial. Data was measured in this work and from Vilas-Boas *et al.*^[3].

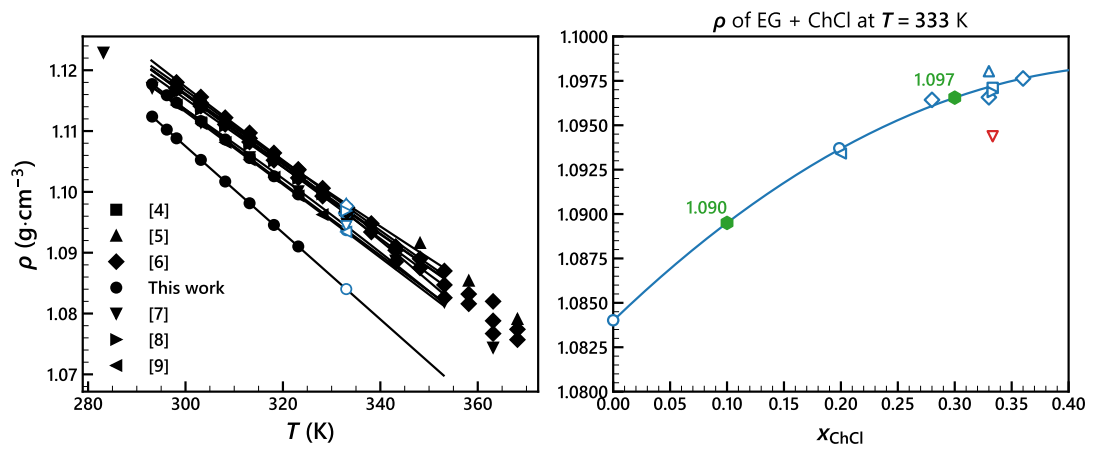


Fig. S4 Estimated densities for ethylene glycol + choline chloride (EG + ChCl) by interpolating the data to 333 K and to $x_{\text{ChCl}} = 0.1$ and $x_{\text{ChCl}} = 0.3$ and using second-order polynomials. Data was measured in this work and from^[4–9]. The data from Yadav *et al.*^[7] (in red) was omitted in the composition-based fit because it does not match the general trend of the other sources or this work.

SI–2 Supplementary Discussion

SI–2.1 Impact of heat capacity change on excess properties

Heat capacity change of fusion. As discussed in the main text, $\Delta_{\text{trs}}C_{p,i}$ significantly impacts SLE-derived G_i^E values. The $\Delta_{\text{trs}}C_{p,i}$ -term is often ignored, but this is only valid over small temperature intervals. Studied mixtures consist of a low-melting compound and a high-melting salt. Hence, the salt's melting point depression is large and the $\Delta_{\text{fus}}C_{p,\text{salt}}$ contribution is significant. It is difficult to obtain accurate data on the salt's liquid heat capacity at temperatures well below its melting point. Therefore, it is commonly assumed that the heat capacities of the liquid and solid change as a function of temperature, but their difference ($\Delta_{\text{fus}}C_{p,\text{salt}}$) is fairly constant. As significant entropy differences between the solid and the liquid phase exist, it remains an approximation. However, it provides a better description of G_i^E than when heat capacities are simply ignored.

Heat capacity data is compiled for a wide variety of compounds, but for some compounds, the pure solid or liquid phase is experimentally difficult to assess. As a result, $\Delta_{\text{fus}}C_{p,\text{salt}}$ (or $\Delta_{\text{trs}}C_{p,\text{salt}}$ for a solid–solid transition) cannot be easily quantified. ChCl thermally decomposes upon heating, rendering its liquid phase inaccessible. We could measure ChCl's melting point and enthalpy of fusion with fast scanning calorimetry for the first time,^[10] but partial decomposition did not allow for the direct measurement of $\Delta_{\text{fus}}C_{p,\text{ChCl}}$.

Instead, we calculated $\Delta_{\text{fus}}C_{p,\text{ChCl}}$ from the data measured by Lobo Ferreira *et al.*^[11]. By linearly extrapolating the heat capacity of various aqueous solutions ($x_{\text{ChCl}} < 0.4$) to pure ChCl, they obtained $C_{p,\text{ChCl}}^l = 249 \pm 10 \text{ J}\cdot\text{mol}^{-1}\cdot\text{K}^{-1}$ at 298.15 K. The heat capacity of ChCl's solid low-temperature polymorph α was measured directly.^[11] From interpolation, we calculated $C_{p,\text{ChCl}}^\alpha = 51.3 + 0.528 * 298.15 = 208.7 \pm 1.8 \text{ J}\cdot\text{mol}^{-1}\cdot\text{K}^{-1}$. They determined $\Delta_{\text{trs}}C_{p,\text{ChCl}} = 20 \pm 3 \text{ J}\cdot\text{mol}^{-1}\cdot\text{K}^{-1}$ at 352.2 K,^[11] and assuming it is temperature independent it follows that:

$$\Delta_{\text{fus}}C_{p,\text{ChCl}} = C_{p,\text{ChCl}}^l - C_{p,\text{ChCl}}^\alpha - \Delta_{\text{trs}}C_{p,\text{ChCl}} = 20.3 \pm 10.6 \text{ J}\cdot\text{mol}^{-1}\cdot\text{K}^{-1}.$$

Partial molar excess Gibbs energy of mixing. Fig. S5 shows how the significant uncertainty in $\Delta_{\text{fus}}C_{p,\text{ChCl}}$ translates into G_i^E . The lowest limit, $\Delta_{\text{fus}}C_{p,\text{ChCl}} = 9.7 \text{ J}\cdot\text{mol}^{-1}\cdot\text{K}^{-1}$, shows a discontinuity in G_{ChCl}^E at the solid–solid transition and is probably too low. The highest limit, $\Delta_{\text{fus}}C_{p,\text{ChCl}} = 30.9 \text{ J}\cdot\text{mol}^{-1}\cdot\text{K}^{-1}$ visually shows consistent behaviour, with the Redlich–Kister fit of $G_{\text{H}_2\text{O}}^E$ passing through the water activity-derived data. From this analysis, we expect the true value $\Delta_{\text{fus}}C_{p,\text{ChCl}}$ to be close to or higher than $20.3 \text{ J}\cdot\text{mol}^{-1}\cdot\text{K}^{-1}$. Note that i) the fit is model-dependent, ii) the impact of uncertainty in the SLE data and ChCl's melting point and fusion enthalpy are not shown, and iii) the composition range of $G_{\text{H}_2\text{O}}^E$ and G_{ChCl}^E is limited.

Partial excess molar enthalpy of mixing. H_i^E data obtained from ITC experiments are unaffected by $\Delta_{\text{trs}}C_{p,i}$, but H_{ChCl}^E is significantly impacted because it is calculated from heats of dissolution corrected for the fusion properties (Eq. 5 in main text). H_{ChCl}^E acts as an anchor point for the ChCl-side of the Redlich–Kister fits of H_i^E , so the thermodynamic analysis of the enthalpy of mixing is also affected. The impact of $\Delta_{\text{trs}}C_{p,i}$ on the fitted H_i^E is shown in Fig. S6.

Total molar excess properties of mixing. G_i^E and H_i^E are both affected by the uncertainty in $\Delta_{\text{fus}}C_{p,\text{ChCl}}$, so their integrated properties are as well. Fig. S7 and S8 show the impact on the total molar excess Gibbs energy and enthalpy of mixing. As mentioned earlier, the lower limit of $\Delta_{\text{fus}}C_{p,\text{ChCl}} = 9.7 \text{ J}\cdot\text{mol}^{-1}\cdot\text{K}^{-1}$ shows thermodynamic inconsistencies in G_i^E , and results

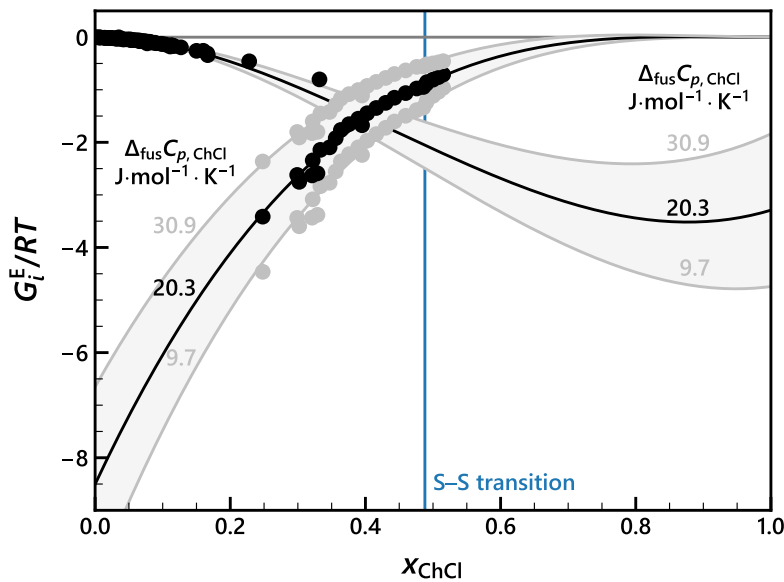


Fig. S5 Normalised partial molar excess Gibbs energy of mixing (G_i^E) for water + choline chloride (ChCl). Values were calculated from solid–liquid equilibrium (SLE) data using $\Delta_{\text{fus}}C_{p,\text{ChCl}} = 20.3 \text{ J}\cdot\text{mol}^{-1}\cdot\text{K}^{-1}$ (black) and 9.7 or $30.9 \text{ J}\cdot\text{mol}^{-1}\cdot\text{K}^{-1}$ (grey) corresponding to the uncertainty limit for $\Delta_{\text{fus}}C_{p,\text{ChCl}}$. In all cases, G_i^E was fitted to a Redlich–Kister (RK) polynomial with two fit parameters. The composition at which the liquidus temperature corresponds to the solid–solid (S–S) transition temperature of ChCl is highlighted in blue.

in favourable H^E for all mixtures and a smaller—but significant—entropy contribution to G^E . The upper limit of $\Delta_{\text{fus}}C_{p,\text{ChCl}} = 30.9 \text{ J}\cdot\text{mol}^{-1}\cdot\text{K}^{-1}$ results in favourable H^E for $\text{H}_2\text{O} + \text{ChCl}$ only. The unfavourable interactions between EG + ChCl and 13PD + ChCl are overcome by a significant S^E contribution. In conclusion, more accurate and precise heat capacity data could significantly improve the calculated thermodynamics of mixing and their interpretation, especially for compounds with a large melting point depression.

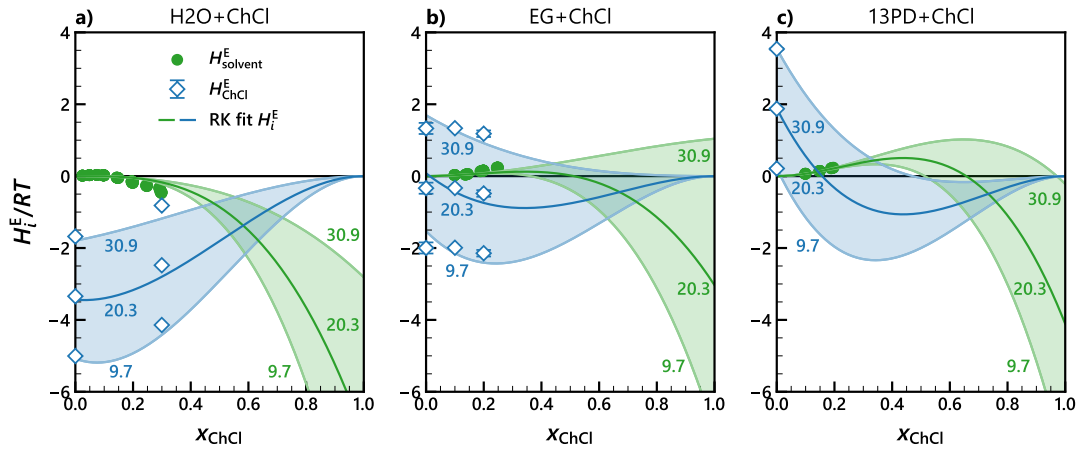


Fig. S6 Normalised partial molar excess enthalpy of mixing (H_i^E/RT) for **a)** water (H_2O) + choline chloride (ChCl), **b)** ethylene glycol (EG) + ChCl , and **c)** 1,3-propanediol (13PD) + ChCl . H_{ChCl}^E (blue) was calculated from isothermal and quasi-adiabatic dissolution calorimetry using $\Delta_{\text{fus}}C_p,\text{ChCl} = 20.3 \text{ J}\cdot\text{mol}^{-1}\cdot\text{K}^{-1}$ and 9.7 or $30.9 \text{ J}\cdot\text{mol}^{-1}\cdot\text{K}^{-1}$ corresponding to the uncertainty limit for $\Delta_{\text{fus}}C_p,\text{ChCl}$. In all cases, H_i^E was fitted to a Redlich–Kister (RK) polynomial with two fitting parameters.

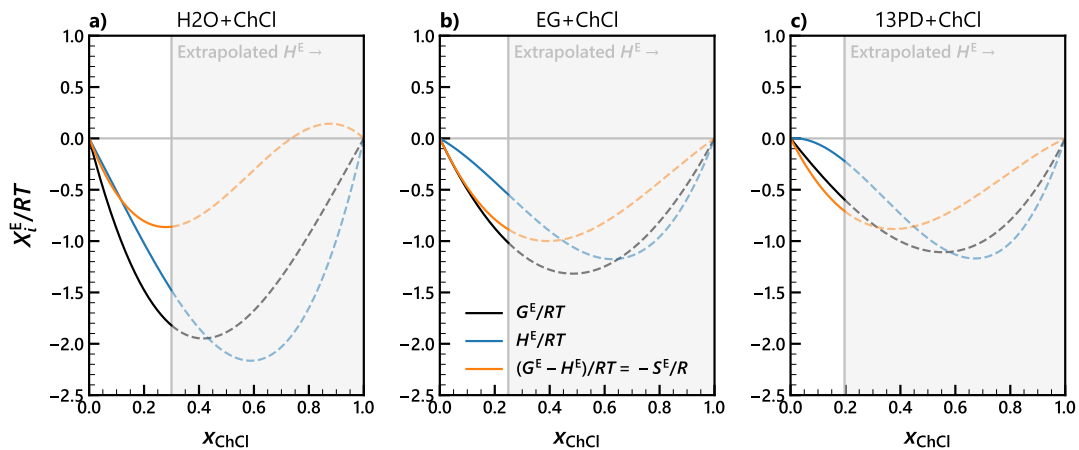


Fig. S7 Normalised molar excess Gibbs energy and enthalpy of mixing (G_i^E/RT and H_i^E/RT) for **a)** water (H_2O) + choline chloride (ChCl), **b)** ethylene glycol (EG) + ChCl , and **c)** 1,3-propanediol (13PD) + ChCl . G_i^E (black) and H_i^E (blue) were calculated from first-order Redlich–Kister fits to their partial molar properties using $\Delta_{\text{fus}}C_p,\text{ChCl} = 9.7 \text{ J}\cdot\text{mol}^{-1}\cdot\text{K}^{-1}$ corresponding to the lowest limit.

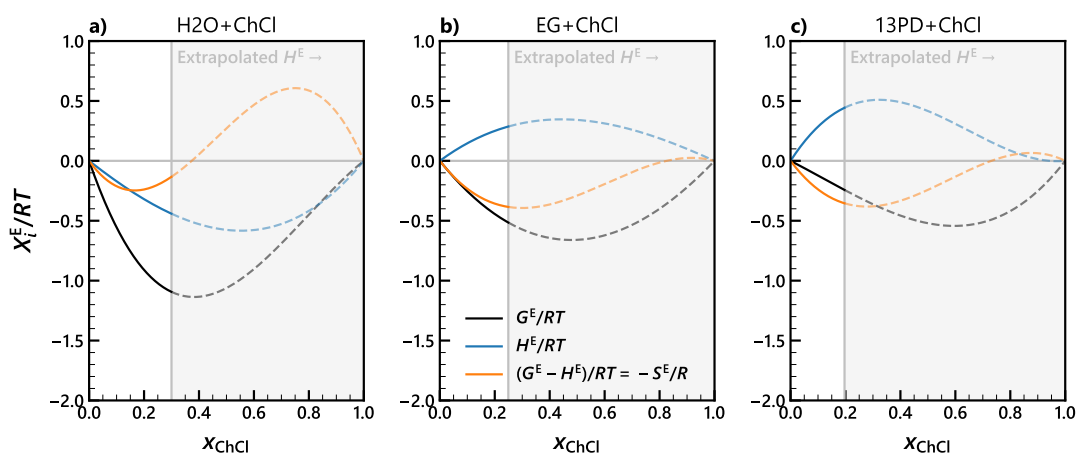


Fig. S8 Normalised molar excess Gibbs energy and enthalpy of mixing (G^E/RT and H^E/RT) for **a)** water (H_2O) + choline chloride (ChCl), **b)** ethylene glycol (EG) + ChCl, and **c)** 1,3-propanediol (13PD) + ChCl. G^E (black) and H^E (blue) were calculated from first-order Redlich–Kister fits to their partial molar properties using $\Delta_{\text{fus}}C_{p,\text{ChCl}} = 30.9 \text{ J}\cdot\text{mol}^{-1}\cdot\text{K}^{-1}$ corresponding to the highest limit.

SI-3 Supplementary Figures

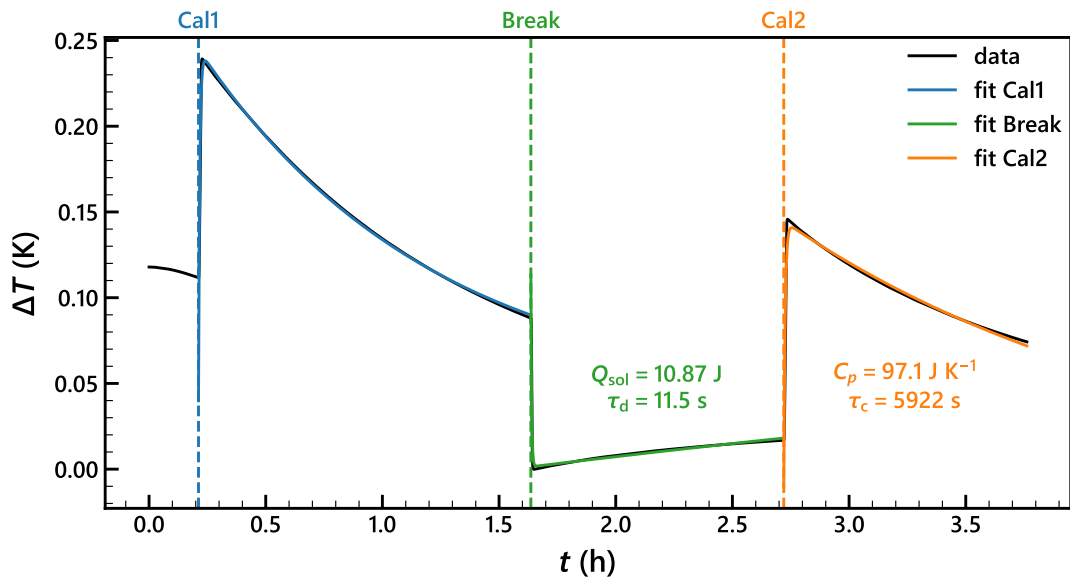


Fig. S9 Temperature profile of the semi-adiabatic dissolution calorimeter for two calibration heat pulses of 15 J and the dissolution of choline chloride (ChCl) in pure H₂O. The heat capacity (C_p) and time constant (τ_c) of the calorimeter were fit to the second calibration to obtain the heat (Q_{sol}) and time constant (τ_d) of dissolution.

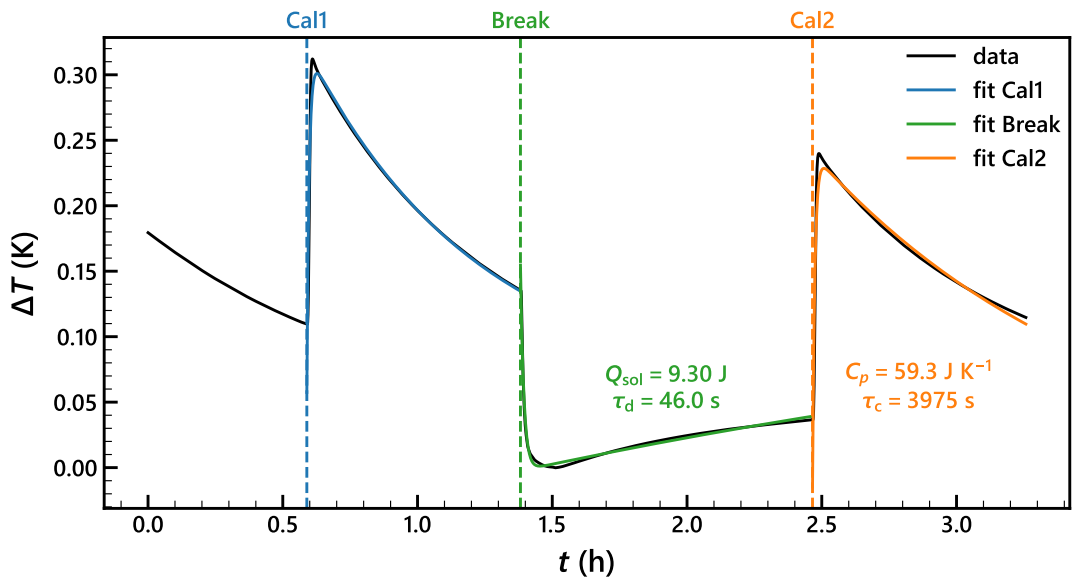


Fig. S10 Temperature profile of the semi-adiabatic dissolution calorimeter for two calibration heat pulses of 15 J and the dissolution of choline chloride (ChCl) in pure H₂O + ChCl at x_{ChCl} . The heat capacity (C_p) and time constant (τ_c) of the calorimeter were fit to the second calibration to obtain the heat (Q_{sol}) and time constant (τ_d) of dissolution.

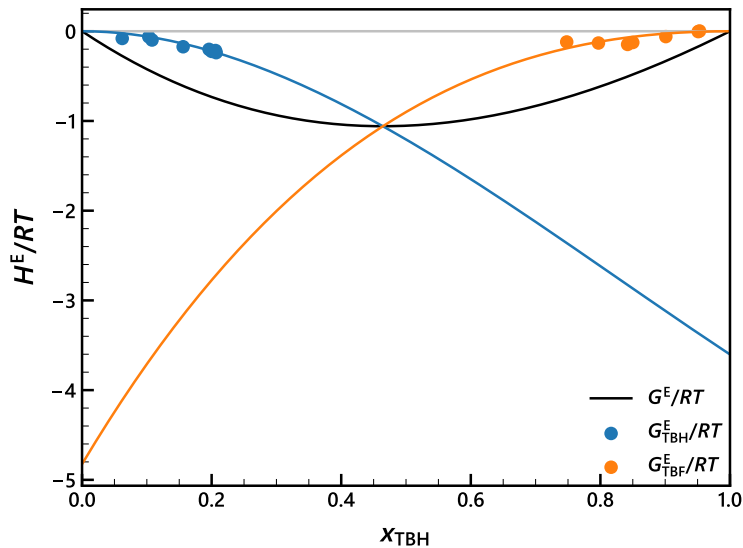


Fig. S11 Normalised partial molar Gibbs excess energies (G_i^E/RT) as calculated from the solid–liquid equilibrium data and fusion properties for tert-butyl alcohol (TBH) + perfluoro-tert-butyl alcohol (TBF) as published by Vaz *et al.*^[12]. Only the points in equilibrium with the pure solid were fitted to a first-order Redlich–Kister polynomial to obtain the equimolar total normalised molar Gibbs excess energy $G^E(x_{\text{TBF}} = 0.5)/RT$.

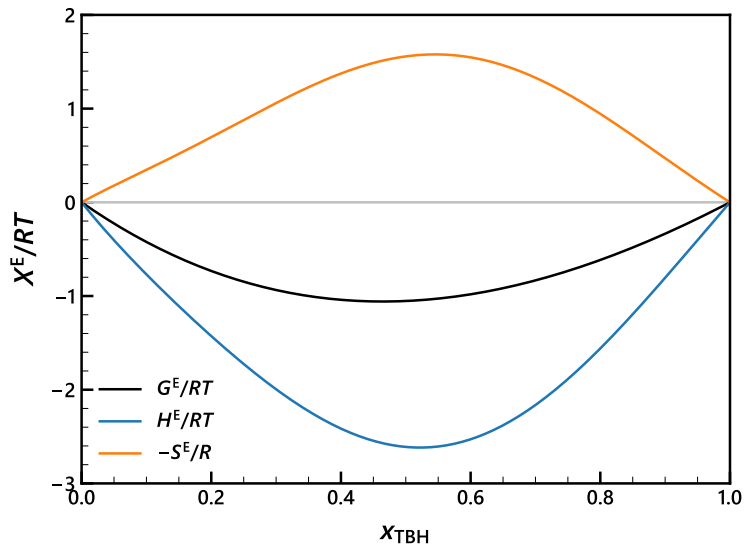


Fig. S12 Normalised molar excess properties as calculated from Fig. S11 and the Redlich–Kister parameters for H^E published by Vaz *et al.*^[12].

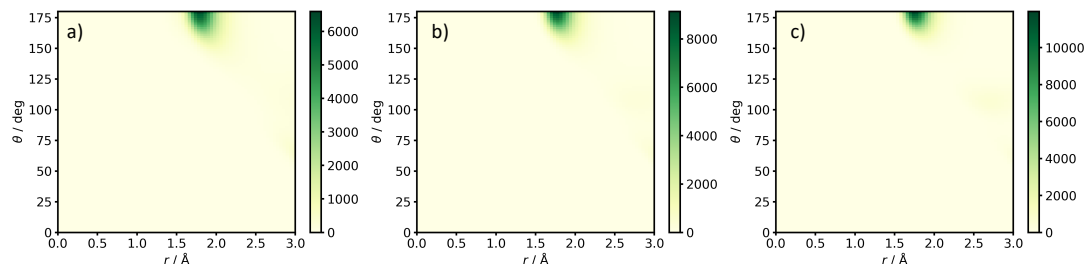


Fig. S13 Combined angle-distance distribution function (CDF) of the $\text{H}_2\text{O}-\text{H}_2\text{O}$ hydrogen bond at a) $x_{\text{ChCl}} = 0.0$ (pure water), b) $x_{\text{ChCl}} = 0.1$ and c) $x_{\text{ChCl}} = 0.3$. The intensities in the lateral color bar represent the counts.

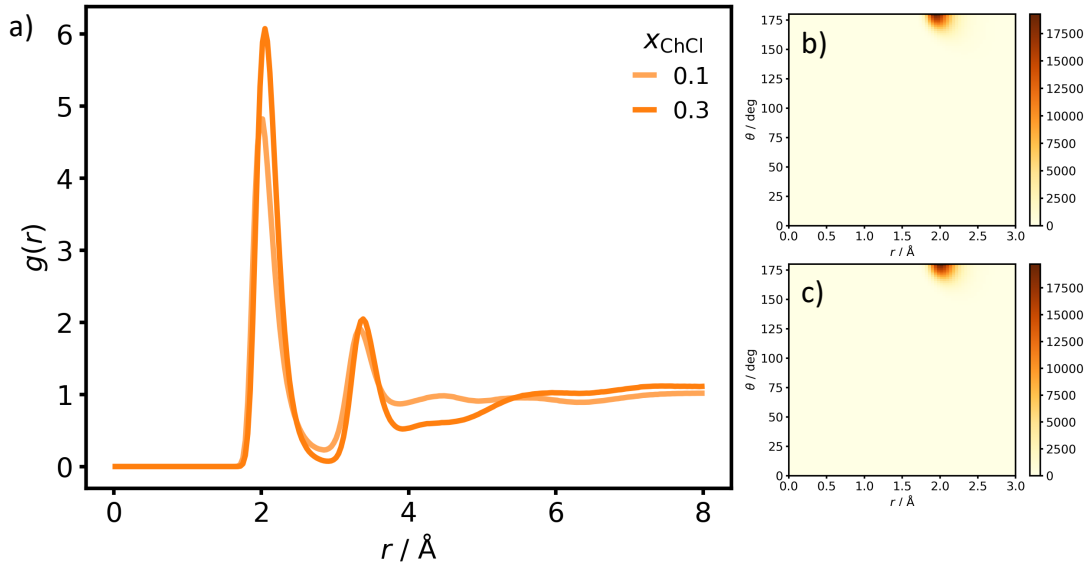


Fig. S14 a) Radial distribution functions (RDFs) of the $\text{H}\cdots\text{Cl}$ distance between the H atom of H_2O and the anion at different concentrations of salt. b) Combined angle-distance distribution function (CDF) of H_2O and Cl at $x_{\text{ChCl}} = 0.1$. c) Combined angle-distance distribution function (CDF) of H_2O and Cl at $x_{\text{ChCl}} = 0.3$. The intensities in the lateral color bar represent the counts.

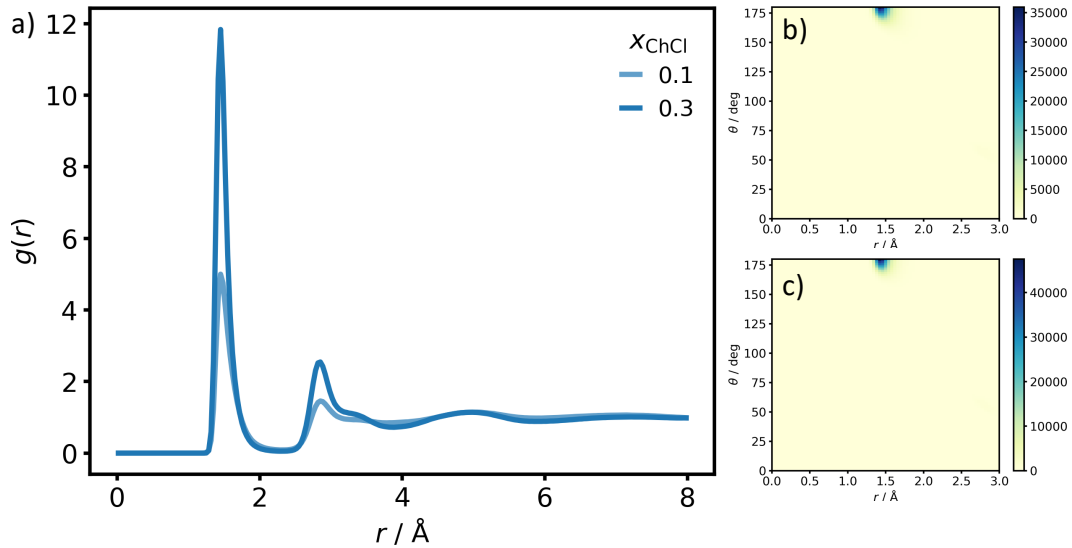


Fig. S15 a) Radial distribution functions (RDFs) of the $\text{H}\cdots\text{O}$ distance between the H atom of H_2O and the O atom of choline at different concentrations of salt. b) Combined angle-distance distribution function (CDF) of H_2O and the O atom of the cation at $x_{\text{ChCl}} = 0.1$. c) Combined angle-distance distribution function (CDF) of H_2O and the O atom of the cation at $x_{\text{ChCl}} = 0.3$. The intensities in the lateral color bar represent the counts.

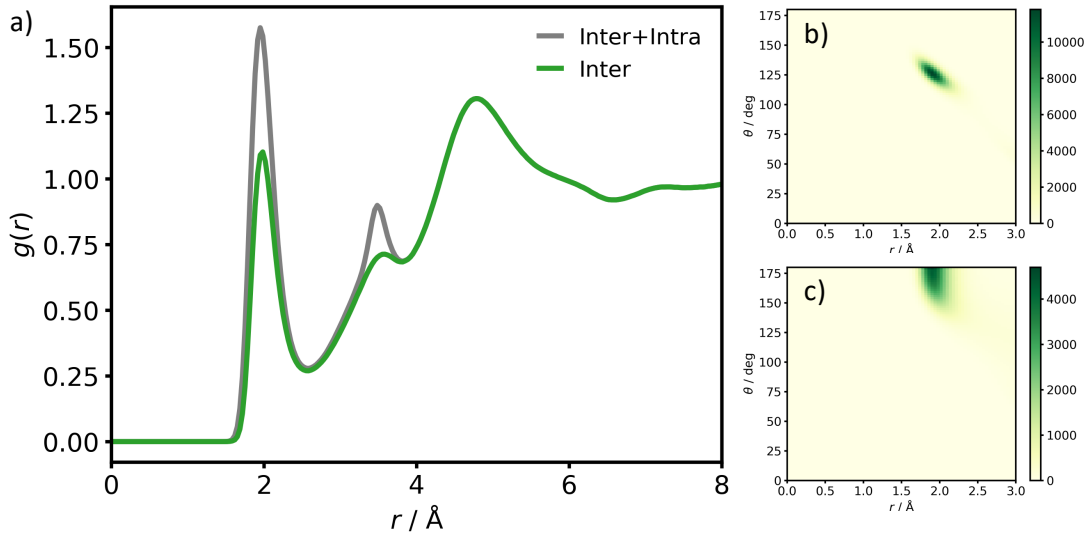


Fig. S16 a) Radial distribution functions (RDFs) of the inter- and intra-molecular $\text{H}\cdots\text{O}$ distance between the hydroxyl groups of EG. b) Combined angle-distance distribution function (CDF) of the intra-molecular H-bond in EG. c) Combined angle-distance distribution function (CDF) of the intra-molecular H-bond in EG. The intensities in the lateral color bar represent the counts.

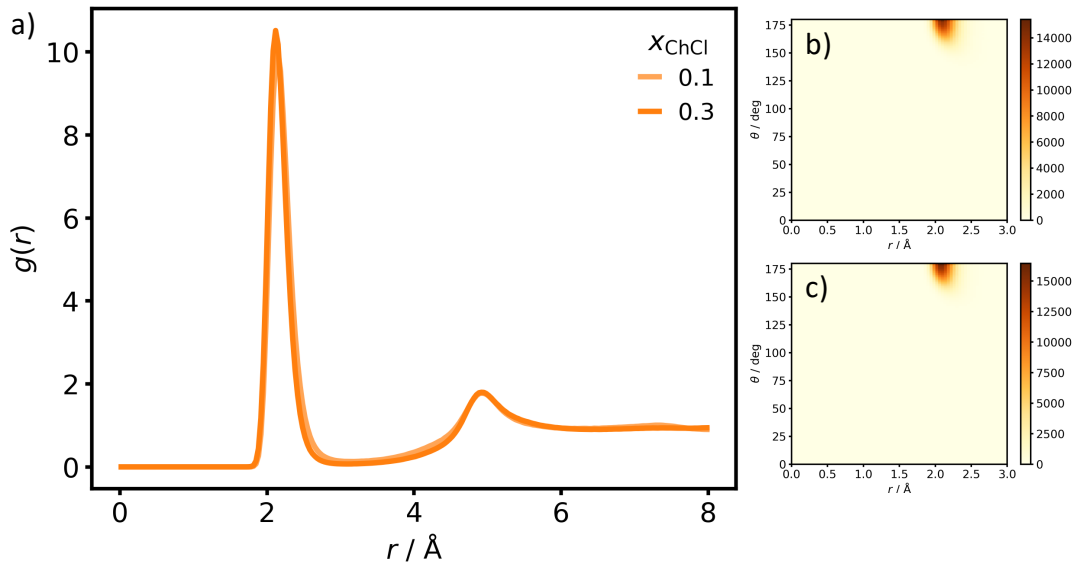


Fig. S17 a) Radial distribution functions (RDFs) of the $\text{H}\cdots\text{Cl}$ distance between the hydroxyl groups of EG and the anion at different concentrations of salt. b) Combined angle-distance distribution function (CDF) of the hydroxyl group of EG and Cl at $x_{\text{ChCl}} = 0.1$. c) Combined angle-distance distribution function (CDF) of the hydroxyl group of EG and Cl at $x_{\text{ChCl}} = 0.3$. The intensities in the lateral color bar represent the counts.

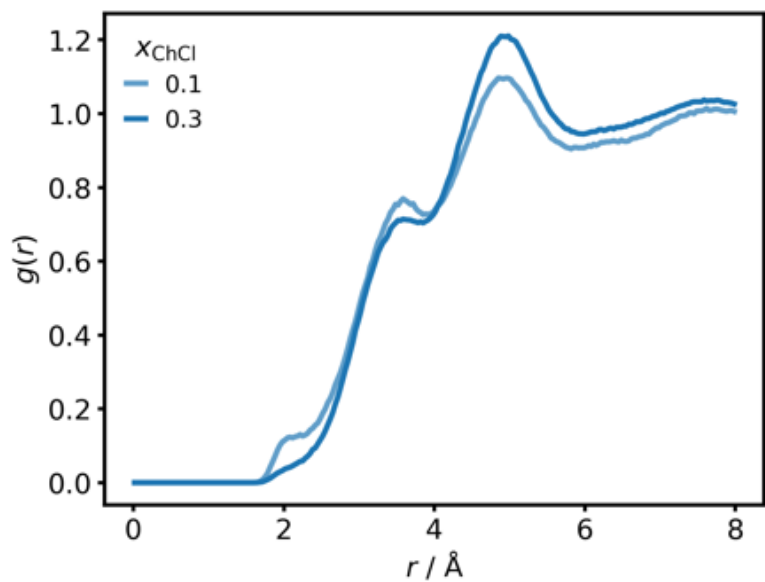


Fig. S18 Radial distribution functions (RDFs) of the intermolecular $\text{H}\cdots\text{O}$ distance between the hydroxyl groups of EG at different concentrations of salt.

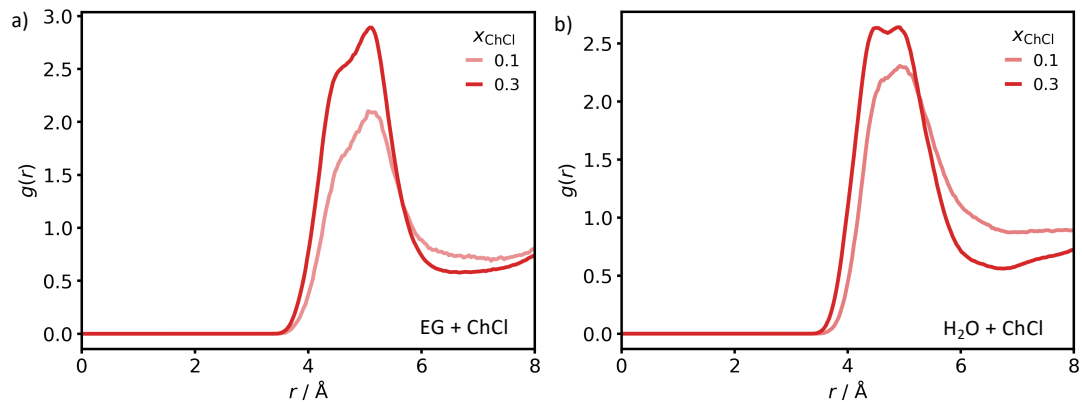


Fig. S19 Radial distribution functions (RDFs) at different concentrations of ChCl between the centers of mass of Ch and Cl a) in EG and b) in H_2O .

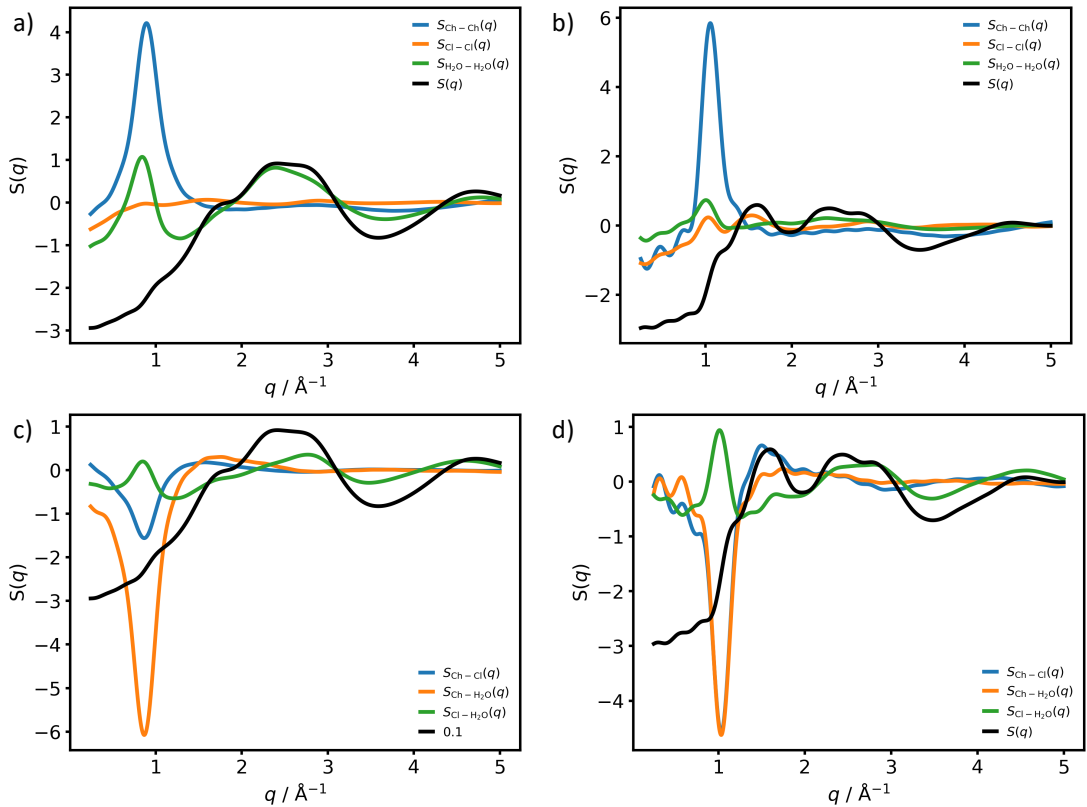


Fig. S20 Simulated X-ray static structure factors of H₂O+ChCl. Total $S(q)$ (black) and partial $S_{\alpha-\beta}(q)$ (colored). a-b) Partial structure factors of like-like correlations, Ch – Ch (blue), Cl – Cl (orange) and H₂O – H₂O (green), at $x_{\text{ChCl}} = 0.1$ and $x_{\text{ChCl}} = 0.3$, respectively. c-d) Partial structure factors of unlike correlations between Ch – Cl (blue), Ch – H₂O (orange) and Cl – H₂O (green).

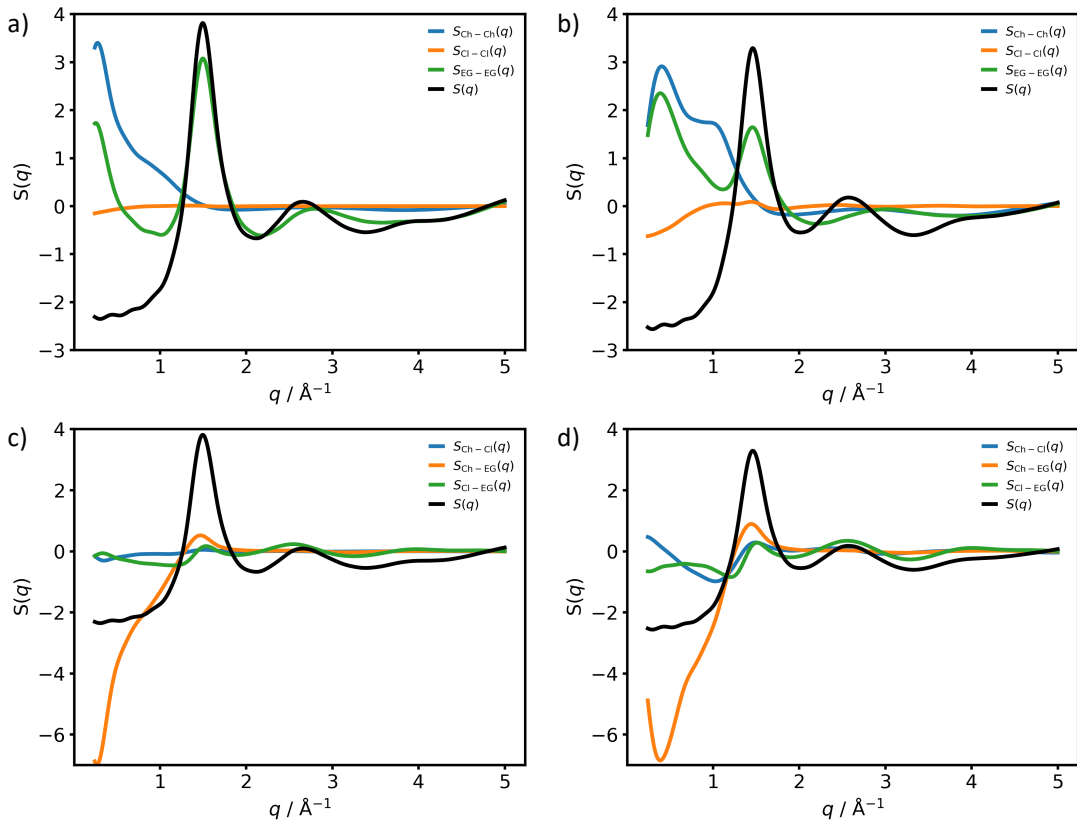


Fig. S21 Simulated X-ray static structure factors of EG+ChCl. Total $S(q)$ (black) and partial $S_{\alpha-\beta}(q)$ (colored). a-b) Partial structure factors of like-like correlations, Ch – Ch (blue), Cl – Cl (orange) and EG – EG (green), at $x_{\text{ChCl}} = 0.1$ and $x_{\text{ChCl}} = 0.3$, respectively. c-d) Partial structure factors of unlike correlations between Ch – Cl (blue), Ch – EG (orange) and Cl – EG (green).

SI–4 Supplementary Tables

Table S4 Thermophysical properties of the pure component phase transitions used to calculate G_i^E from solid–liquid equilibrium data. T_{trs} is the transition temperature, $\Delta_{trs}H$ is the enthalpy of transition, and $\Delta_{trs}C_p$ is the heat capacity change of transition at constant pressure. DSC refers to differential scanning calorimetry measurements from this work.

component	transition	T_{trs} K	$\Delta_{trs}H$ $J \cdot mol^{-1}$	$\Delta_{trs}C_p$ $J \cdot mol^{-1} \cdot K^{-1}$	Ref
water	fusion	273.16	6008	38.2	[13]
ethylene glycol	fusion	260.3	9500	44	DSC, [14–16]
choline chloride	fusion	687	13800	20.3	[10,11]
	solid–solid	352.2	16300	20.0	[11]

Table S5 Normalised partial molar excess Gibbs energy of mixing of water ($G_{H_2O}^E/RT$) at 298.15 K calculated from osmotic coefficient data on molality basis (Φ_m) as a function of choline chloride mole fraction (x_{ChCl}) published by Macaskill *et al.*^[17].

x_{ChCl}	Φ_m	$G_{H_2O}^E/RT$	x_{ChCl}	Φ_m	$G_{H_2O}^E/RT$
0.00266	0.8979	-0.00213	0.05136	0.9060	-0.04538
0.00575	0.8760	-0.00436	0.05320	0.9123	-0.04786
0.00790	0.8641	-0.00583	0.05777	0.9257	-0.05401
0.01397	0.8526	-0.01009	0.06213	0.9383	-0.06018
0.01721	0.8525	-0.01250	0.06416	0.9422	-0.06288
0.02153	0.8537	-0.01580	0.06666	0.9531	-0.06715
0.02193	0.8539	-0.01611	0.06719	0.9508	-0.06742
0.02405	0.8535	-0.01772	0.07223	0.9652	-0.07532
0.02649	0.8580	-0.01985	0.07446	0.9741	-0.07935
0.02934	0.8632	-0.02240	0.07790	0.9907	-0.08629
0.03134	0.8663	-0.02422	0.08225	1.0056	-0.09441
0.03449	0.8698	-0.02704	0.08800	1.0233	-0.10536
0.03743	0.8766	-0.03002	0.09770	1.0527	-0.12516
0.04020	0.8814	-0.03281	0.10462	1.0754	-0.14080
0.04757	0.8999	-0.04116	0.11374	1.1030	-0.16237

Table S6 Normalised partial molar excess Gibbs energy of mixing of water ($G_{\text{H}_2\text{O}}^{\text{E}}/RT$) at 298.15 K calculated from water activity data ($a_{\text{H}_2\text{O}}$) as a function of choline chloride mole fraction (x_{ChCl}) published by Khan *et al.*^[18].

x_{ChCl}	$a_{\text{H}_2\text{O}}$	$G_{\text{H}_2\text{O}}^{\text{E}}/RT$
0.015	0.972	-0.013
0.031	0.944	-0.025
0.052	0.906	-0.046
0.080	0.844	-0.087
0.113	0.762	-0.152
0.160	0.648	-0.259
0.228	0.488	-0.459
0.332	0.299	-0.803

Table S7 Solid–liquid equilibrium data of water (H_2O) + choline chloride (ChCl). Tabulated are the liquidus temperature (T_{liq}) and the normalised partial molar excess Gibbs energy (G_i^{E}/RT) calculated from it as a function of ChCl mole fraction (x_{ChCl}). The literature source (Ref) or differential scanning calorimetry (DSC, this work) is mentioned for the T_{liq} data, and $G_{\text{ChCl}}^{\text{E}}/RT$ was calculated using four different values for ChCl the heat capacity change of fusion (ΔC_p in $\text{J}\cdot\text{mol}^{-1}\cdot\text{K}^{-1}$).

x_{ChCl}	T_{liq} K	Ref	$G_{\text{H}_2\text{O}}^{\text{E}}/RT$	x_{ChCl}	T_{liq} K	Ref	$G_{\text{ChCl}}^{\text{E}}/RT$				
							0	9.7	20.3	30.9	$\leftarrow \Delta C_p$
0.0350	269.2	DSC	-0.003	0.3470	285.5	DSC	-3.423	-2.769	-2.096	-1.422	
0.0000	273.1	[3]	-0.000	0.3636	298.1	[3]	-2.932	-2.363	-1.765	-1.166	
0.0070	271.7	[11]	-0.007	0.3757	303.1	[3]	-2.764	-2.226	-1.654	-1.083	
0.0140	270.5	[11]	-0.012	0.3894	308.1	[3]	-2.606	-2.096	-1.551	-1.005	
0.0230	269.1	[11]	-0.016	0.4025	313.1	[3]	-2.452	-1.968	-1.447	-0.927	
0.0320	267.3	[11]	-0.024	0.4160	318.1	[3]	-2.303	-1.843	-1.347	-0.850	
0.0420	264.2	[11]	-0.044	0.4299	323.1	[3]	-2.160	-1.723	-1.249	-0.775	
0.0540	261.6	[11]	-0.057	0.4429	328.1	[3]	-2.019	-1.604	-1.152	-0.699	
0.0660	258.3	[11]	-0.077	0.4595	333.1	[3]	-1.890	-1.495	-1.063	-0.632	
0.0830	253.9	[11]	-0.101	0.4758	338.1	[3]	-1.764	-1.388	-0.976	-0.565	
0.0900	251.8	[11]	-0.114	0.4857	343.1	[3]	-1.699	-1.340	-0.947	-0.555	
0.1000	249.0	[11]	-0.131	0.2480	238.4	[11]	-5.592	-4.463	-3.414	-2.364	
0.1170	243.3	[11]	-0.168	0.2990	264.8	[11]	-4.265	-3.437	-2.620	-1.803	
0.1270	239.6	[11]	-0.193	0.3020	261.3	[11]	-4.458	-3.596	-2.752	-1.907	
0.1500	230.2	[11]	-0.260	0.3210	266.6	[11]	-4.244	-3.433	-2.630	-1.826	
0.1660	223.3	[11]	-0.309	0.3220	275.3	[11]	-3.818	-3.084	-2.343	-1.603	
0.0769	252.9	[19]	-0.117	0.3290	268.5	[11]	-4.172	-3.379	-2.590	-1.801	
0.1111	243.1	[19]	-0.177	0.3560	292.1	[11]	-3.162	-2.554	-1.921	-1.288	
0.1667	219.9	[19]	-0.341	0.3950	304.2	[11]	-2.773	-2.241	-1.675	-1.109	
0.0902	254.3	[20]	-0.089	0.4900	353.2	[11]	-1.570	-1.244	-0.887	-0.530	
0.1238	239.2	[20]	-0.201	0.4910	358.2	[11]	-1.506	-1.195	-0.855	-0.515	
0.1419	233.7	[20]	-0.235	0.5000	368.2	[11]	-1.399	-1.116	-0.808	-0.499	
0.1665	218.3	[20]	-0.357	0.5080	378.2	[11]	-1.295	-1.039	-0.759	-0.479	
				0.5150	388.2	[11]	-1.196	-0.964	-0.710	-0.457	
				0.3333	282.6	[19]	-3.510	-2.835	-2.144	-1.452	
				0.3320	278.2	[20]	-3.711	-3.001	-2.281	-1.560	

Table S8 Solid–liquid equilibrium data of ethylene glycol (EG) + choline chloride (ChCl). Tabulated are the liquidus temperature (T_{liq}) and the normalised partial molar excess Gibbs energy (G_i^{E}/RT) calculated from it as a function of ChCl mole fraction (x_{ChCl}). The literature source (Ref) or differential scanning calorimetry (DSC, this work) is mentioned for the T_{liq} data, and $G_{\text{ChCl}}^{\text{E}}/RT$ was calculated using four different values for ChCl the heat capacity change of fusion (ΔC_p in $\text{J}\cdot\text{mol}^{-1}\cdot\text{K}^{-1}$).

x_{ChCl}	T_{liq}	Ref	$G_{\text{EG}}^{\text{E}}/RT$	x_{ChCl}	T_{liq}	Ref	$G_{\text{ChCl}}^{\text{E}}/RT$				$\leftarrow \Delta C_p$
							0	9.7	20.3	30.9	
0.0373	256.7	DSC	-0.047	0.1755	252.3	DSC	-4.625	-3.634	-2.714	-1.795	
0.0749	254.0	DSC	-0.063	0.1917	256.5	DSC	-4.478	-3.535	-2.651	-1.768	
0.0996	251.5	DSC	-0.090	0.2498	274.7	DSC	-3.812	-3.049	-2.304	-1.559	
0.1501	247.7	DSC	-0.115	0.3035	291.4	DSC	-3.248	-2.619	-1.981	-1.344	
0.0000	260.3	[21]	-0.010	0.3538	307.6	DSC	-2.749	-2.225	-1.676	-1.128	
0.0440	260.7	[21]	0.043	0.3897	329.6	DSC	-2.059	-1.645	-1.199	-0.753	
0.0930	255.8	[21]	-0.006	0.4515	342.9	DSC	-1.780	-1.419	-1.026	-0.633	
0.1150	254.6	[21]	-0.007	0.1850	257.2	[21]	-4.406	-3.470	-2.592	-1.714	
0.1370	251.5	[21]	-0.047	0.2170	265.3	[21]	-4.136	-3.285	-2.471	-1.658	
0.1610	251.6	[21]	-0.017	0.2480	275.6	[21]	-3.759	-3.005	-2.266	-1.527	
				0.2910	288.7	[21]	-3.323	-2.674	-2.020	-1.367	
				0.3330	304.9	[21]	-2.792	-2.251	-1.689	-1.127	

Table S9 Solid–liquid equilibrium data of 1,3-propanediol + choline chloride (ChCl). Tabulated are the liquidus temperature (T_{liq}) and the normalised partial molar excess Gibbs energy (G_i^{E}/RT) calculated from it as a function of ChCl mole fraction (x_{ChCl}). The T_{liq} data was measured with differential scanning calorimetry (DSC) in this work), and $G_{\text{ChCl}}^{\text{E}}/RT$ was calculated using four different values for ChCl the heat capacity change of fusion (ΔC_p in $\text{J}\cdot\text{mol}^{-1}\cdot\text{K}^{-1}$).

x_{ChCl}	T_{liq}	$G_{\text{ChCl}}^{\text{E}}/RT$					$\leftarrow \Delta C_p$
		K	0	9.7	20.3	30.9	
0.1000	252.7	-4.040	-3.054	-2.138	-1.222		
0.1250	259.1	-3.913	-2.997	-2.135	-1.272		
0.1500	266.5	-3.707	-2.868	-2.063	-1.258		
0.2000	279.0	-3.383	-2.657	-1.942	-1.227		
0.3000	301.7	-2.813	-2.253	-1.674	-1.095		

Table S10 Isothermal titration calorimetry data for water (1) + choline chloride (2) at 298.15 K. Where n_i are the number of moles of i in the cell (subscript c) or syringe (subscript s), and Q is the heat flow integral for each injection.

$x_{2,c}$	$n_{1,c}$ mmol	$n_{2,c}$ mmol	$n_{1,s}$ μmol	$n_{2,s}$ μmol	Q mJ
0.0002	49.898	0.012	28.038	11.999	19.99
0.0005	49.926	0.024	13.835	5.920	9.79
0.0006	49.939	0.030	56.459	24.161	37.93
0.0011	49.996	0.054	13.835	5.920	9.11
0.0012	50.010	0.060	13.835	5.920	8.76
0.0013	50.024	0.066	13.835	5.920	8.61
0.0014	50.037	0.072	13.835	5.920	8.14
0.0016	50.051	0.078	13.835	5.920	8.07
0.0017	50.065	0.084	13.835	5.920	8.05
0.0018	50.079	0.090	13.835	5.920	7.77
0.0002	48.127	0.012	28.038	11.999	21.75
0.0005	48.155	0.024	28.038	11.999	21.38
0.0007	48.183	0.036	28.038	11.999	21.80
0.0010	48.211	0.048	28.038	11.999	21.16
0.0012	48.239	0.060	28.038	11.999	20.08
0.0015	48.267	0.072	28.038	11.999	19.26
0.0017	48.295	0.084	28.038	11.999	18.59
0.0020	48.323	0.096	28.038	11.999	18.62
0.0022	48.351	0.108	28.038	11.999	17.87
0.0025	48.379	0.120	28.038	11.999	17.25
0.0027	48.407	0.132	28.038	11.999	16.49
0.0030	48.435	0.144	28.038	11.999	16.16
0.0032	48.463	0.156	28.038	11.999	15.46
0.0035	48.491	0.168	28.038	11.999	14.79
0.0037	48.519	0.180	28.038	11.999	14.37
0.0039	48.547	0.192	28.038	11.999	14.26
0.0042	48.575	0.204	28.038	11.999	13.21
0.0044	48.603	0.216	28.038	11.999	12.66
0.0047	48.632	0.228	28.038	11.999	12.02
0.0049	48.660	0.240	28.038	11.999	11.70
0.0051	48.688	0.252	28.038	11.999	11.12
0.0054	48.716	0.264	28.038	11.999	10.55
0.0056	48.744	0.276	28.038	11.999	10.20
0.0059	48.772	0.288	28.038	11.999	10.50
0.0061	48.800	0.300	28.038	11.999	9.15
0.0063	48.828	0.312	28.038	11.999	8.80
0.0066	48.856	0.324	28.038	11.999	8.22
0.0068	48.884	0.336	28.038	11.999	7.93
0.0071	48.912	0.348	28.038	11.999	7.47
0.0073	48.940	0.360	28.038	11.999	7.08
0.0075	48.968	0.372	28.038	11.999	6.68
0.0242	42.667	1.057	165.533	0	4.98

Continued on next page

Table S10 – continued from previous page

$x_{2,c}$	$n_{1,c}$ mmol	$n_{2,c}$ mmol	$n_{1,s}$ μmol	$n_{2,s}$ μmol	Q mJ
0.0243	42.501	1.057	165.533	0	5.38
0.0244	42.336	1.057	165.533	0	5.62
0.0245	42.170	1.057	165.533	0	5.11
0.0245	42.005	1.057	165.533	0	7.09
0.0246	41.839	1.057	165.533	0	5.29
0.0247	41.674	1.057	165.533	0	5.36
0.0248	41.508	1.057	165.533	0	5.29
0.0249	41.343	1.057	165.533	0	5.29
0.0478	37.219	1.870	137.686	0	9.12
0.0480	37.081	1.870	137.686	0	9.11
0.0482	36.943	1.870	137.686	0	9.17
0.0483	36.806	1.870	137.686	0	9.18
0.0485	36.668	1.870	137.686	0	9.23
0.0487	36.530	1.870	137.686	0	9.67
0.0489	36.393	1.870	137.686	0	8.38
0.0490	36.255	1.870	137.686	0	9.51
0.0492	36.117	1.870	137.686	0	9.39
0.0494	35.979	1.870	137.686	0	9.45
0.0496	35.842	1.870	137.686	0	9.37
0.0498	35.704	1.870	137.686	0	8.96
0.0738	100.681	8.025	275.372	0	23.60
0.0740	100.406	8.025	275.372	0	23.04
0.0742	100.130	8.025	275.372	0	23.19
0.0744	99.855	8.025	275.372	0	23.98
0.0746	99.580	8.025	275.372	0	23.07
0.0748	99.304	8.025	275.372	0	24.51
0.0750	99.029	8.025	275.372	0	23.67
0.0939	28.623	2.966	109.839	0	7.17
0.0942	28.513	2.966	109.839	0	6.96
0.0946	28.403	2.966	109.839	0	6.79
0.0949	28.293	2.966	109.839	0	6.60
0.0952	28.184	2.966	109.839	0	6.81
0.0956	28.074	2.966	109.839	0	6.67
0.0959	27.964	2.966	109.839	0	6.64
0.0962	27.854	2.966	109.839	0	6.59
0.0966	27.744	2.966	109.839	0	6.60
0.0969	27.634	2.966	109.839	0	6.45
0.0973	27.525	2.966	109.839	0	6.43
0.0976	27.415	2.966	109.839	0	6.54
0.0980	27.305	2.966	109.839	0	6.81
0.0983	27.195	2.966	109.839	0	7.06
0.0987	27.085	2.966	109.839	0	6.90
0.0991	26.975	2.966	109.839	0	6.68
0.0994	26.866	2.966	109.839	0	6.47

Continued on next page

Table S10 – continued from previous page

$x_{2,c}$	$n_{1,c}$ mmol	$n_{2,c}$ mmol	$n_{1,s}$ μmol	$n_{2,s}$ μmol	Q mJ
0.0996	26.811	2.966	54.197	0	3.25
0.0972	98.452	10.603	275.372	0	17.19
0.0975	98.176	10.603	275.372	0	16.37
0.0977	97.901	10.603	275.372	0	16.97
0.0980	97.626	10.603	275.372	0	16.69
0.0982	97.350	10.603	275.372	0	16.45
0.0985	97.075	10.603	275.372	0	16.23
0.0987	96.799	10.603	275.372	0	15.42
0.0990	96.524	10.603	275.372	0	16.35
0.0992	96.249	10.603	275.372	0	16.62
0.0995	95.973	10.603	275.372	0	15.47
0.0997	95.698	10.603	275.372	0	15.58
0.0999	26.798	2.975	13.835	5.920	-10.79
0.1001	26.812	2.981	13.835	5.920	-10.99
0.1002	26.826	2.987	13.835	5.920	-11.95
0.1003	26.839	2.993	13.835	5.920	-11.85
0.1005	26.853	2.999	13.835	5.920	-12.00
0.1006	26.867	3.005	13.835	5.920	-12.00
0.1007	26.881	3.011	13.835	5.920	-12.07
0.1009	26.895	3.017	13.835	5.920	-11.95
0.1010	26.909	3.023	13.835	5.920	-11.60
0.1011	26.922	3.029	13.835	5.920	-12.10
0.1012	26.936	3.034	13.835	5.920	-11.82
0.1014	26.950	3.040	13.835	5.920	-11.79
0.1001	26.898	2.993	13.826	5.927	-12.57
0.1003	26.912	2.999	13.826	5.927	-12.79
0.1004	26.926	3.005	13.826	5.927	-12.51
0.1005	26.940	3.011	13.826	5.927	-12.68
0.1007	26.954	3.017	13.826	5.927	-12.65
0.1008	26.967	3.023	13.826	5.927	-12.56
0.1009	26.981	3.029	13.826	5.927	-12.41
0.1011	26.995	3.035	13.826	5.927	-12.32
0.1012	27.009	3.041	13.826	5.927	-12.39
0.1013	27.023	3.046	13.826	5.927	-12.39
0.1014	27.036	3.052	13.826	5.927	-12.32
0.1016	27.050	3.058	13.826	5.927	-13.16
0.1017	27.064	3.064	13.826	5.927	-12.63
0.1018	27.078	3.070	13.826	5.927	-12.86
0.1020	27.092	3.076	13.826	5.927	-12.70
0.1021	27.106	3.082	13.826	5.927	-12.18
0.1002	26.937	2.999	40.606	10.154	-8.33
0.1003	26.978	3.009	40.606	10.154	-8.16
0.1005	27.018	3.019	40.606	10.154	-8.23
0.1007	27.059	3.029	40.606	10.154	-8.31

Continued on next page

Table S10 – continued from previous page

$x_{2,c}$	$n_{1,c}$ mmol	$n_{2,c}$ mmol	$n_{1,s}$ μmol	$n_{2,s}$ μmol	Q mJ
0.1008	27.099	3.039	40.606	10.154	-8.15
0.1010	27.140	3.049	40.606	10.154	-8.42
0.1012	27.181	3.060	40.606	10.154	-8.36
0.1013	27.221	3.070	40.606	10.154	-8.25
0.1429	22.051	3.676	109.839	0	-10.70
0.1435	21.941	3.676	109.839	0	-11.28
0.1441	21.831	3.676	109.839	0	-11.45
0.1448	21.721	3.676	109.839	0	-11.75
0.1454	21.612	3.676	109.839	0	-12.13
0.1460	21.502	3.676	109.839	0	-12.35
0.1467	21.392	3.676	109.839	0	-12.89
0.1473	21.282	3.676	109.839	0	-13.17
0.1480	21.172	3.676	109.839	0	-13.49
0.1486	21.062	3.676	109.839	0	-13.85
0.1493	20.953	3.676	109.839	0	-14.33
0.1944	17.563	4.239	54.197	0	-20.94
0.1949	17.509	4.239	54.197	0	-20.58
0.1954	17.454	4.239	54.197	0	-20.68
0.1959	17.400	4.239	54.197	0	-21.64
0.1964	17.346	4.239	54.197	0	-21.11
0.1969	17.292	4.239	54.197	0	-21.46
0.1974	17.238	4.239	54.197	0	-21.96
0.1979	17.183	4.239	54.197	0	-21.32
0.1984	17.129	4.239	54.197	0	-21.56
0.1989	17.075	4.239	54.197	0	-20.98
0.1994	17.021	4.239	54.197	0	-21.20
0.1961	60.998	14.881	165.533	0	-70.16
0.1965	60.833	14.881	165.533	0	-74.22
0.1970	60.667	14.881	165.533	0	-72.26
0.1974	60.502	14.881	165.533	0	-74.87
0.1978	60.336	14.881	165.533	0	-74.30
0.1983	60.171	14.881	165.533	0	-73.10
0.1987	60.005	14.881	165.533	0	-76.68
0.1992	59.840	14.881	165.533	0	-73.61
0.1996	59.674	14.881	165.533	0	-78.37
0.1953	62.278	15.118	165.533	0	-55.79
0.1958	62.112	15.118	165.533	0	-57.40
0.1962	61.947	15.118	165.533	0	-59.23
0.1966	61.781	15.118	165.533	0	-59.40
0.1970	61.616	15.118	165.533	0	-62.47
0.1974	61.450	15.118	165.533	0	-60.44
0.1979	61.285	15.118	165.533	0	-62.79
0.1983	61.119	15.118	165.533	0	-62.70
0.1987	60.954	15.118	165.533	0	-65.10

Continued on next page

Table S10 – continued from previous page

$x_{2,c}$	$n_{1,c}$ mmol	$n_{2,c}$ mmol	$n_{1,s}$ μmol	$n_{2,s}$ μmol	Q mJ
0.1992	60.788	15.118	165.533	0	-66.53
0.1996	60.622	15.118	165.533	0	-67.15
0.1978	17.442	4.301	62.423	6.936	-12.07
0.1981	17.380	4.294	62.423	6.936	-11.27
0.1984	17.317	4.287	62.423	6.936	-11.36
0.1988	17.255	4.280	62.423	6.936	-11.94
0.1991	17.192	4.273	62.423	6.936	-11.14
0.1994	17.130	4.266	62.423	6.936	-11.78
0.1997	17.068	4.259	62.423	6.936	-11.95
0.1972	17.572	4.316	62.423	6.936	-11.01
0.1975	17.509	4.309	62.423	6.936	-10.76
0.1978	17.447	4.302	62.423	6.936	-10.26
0.1981	17.384	4.295	62.423	6.936	-11.19
0.1984	17.322	4.288	62.423	6.936	-11.09
0.1988	17.260	4.281	62.423	6.936	-11.53
0.1991	17.197	4.274	62.423	6.936	-11.41
0.1994	17.135	4.267	62.423	6.936	-11.41
0.1997	17.072	4.260	62.423	6.936	-11.35
0.2000	16.980	4.245	28.038	11.999	-6.77
0.2003	17.047	4.269	35.125	15.057	-8.53
0.2005	17.082	4.284	35.125	15.057	-8.47
0.2007	17.117	4.299	35.125	15.057	-8.47
0.2010	17.152	4.314	35.125	15.057	-8.62
0.2014	17.222	4.344	35.125	15.057	-8.60
0.2017	17.257	4.359	35.125	15.057	-8.68
0.2019	17.292	4.374	35.125	15.057	-8.52
0.1992	17.415	4.333	78.249	8.694	-11.72
0.1996	17.337	4.325	78.249	8.694	-11.82
0.2000	17.259	4.316	78.249	8.694	-12.02
0.2005	17.180	4.307	78.249	8.694	-11.80
0.2009	17.102	4.299	78.249	8.694	-12.11
0.2013	17.024	4.290	78.249	8.694	-11.87
0.2017	16.946	4.281	78.249	8.694	-12.49
0.2449	14.156	4.591	54.197	0	-34.62
0.2456	14.102	4.591	54.197	0	-34.99
0.2463	14.048	4.591	54.197	0	-36.27
0.2470	13.993	4.591	54.197	0	-36.77
0.2478	13.939	4.591	54.197	0	-37.48
0.2485	13.885	4.591	54.197	0	-36.99
0.2492	13.831	4.591	54.197	0	-33.95
0.2902	12.087	4.941	54.197	0	-44.56
0.2911	12.033	4.941	54.197	0	-44.47
0.2920	11.979	4.941	54.197	0	-44.01
0.2929	11.924	4.941	54.197	0	-47.62

Continued on next page

Table S10 – continued from previous page

$x_{2,c}$	$n_{1,c}$ mmol	$n_{2,c}$ mmol	$n_{1,s}$ μmol	$n_{2,s}$ μmol	Q mJ
0.2939	11.870	4.941	54.197	0	-48.02
0.2948	11.816	4.941	54.197	0	-56.16
0.2958	11.762	4.941	54.197	0	-59.34
0.2968	11.708	4.941	54.197	0	-59.44
0.2977	11.653	4.941	54.197	0	-61.96
0.2987	11.599	4.941	54.197	0	-63.96
0.2922	44.599	18.413	156.498	17.389	-97.07
0.2927	44.442	18.396	156.498	17.389	-98.92
0.2933	44.286	18.378	156.498	17.389	-100.97
0.2938	44.129	18.361	156.498	17.389	-101.14
0.2939	44.099	18.358	30.801	3.422	-18.45
0.2945	43.942	18.340	156.498	17.389	-102.49
0.2950	43.786	18.323	156.498	17.389	-102.84
0.2956	43.629	18.305	156.498	17.389	-102.19
0.2961	43.473	18.288	156.498	17.389	-103.28
0.2967	43.316	18.271	156.498	17.389	-104.14
0.2972	43.160	18.253	156.498	17.389	-103.78
0.2978	43.003	18.236	156.498	17.389	-103.48
0.2983	42.847	18.219	156.498	17.389	-103.56
0.2989	42.690	18.201	156.498	17.389	-104.99
0.2995	42.534	18.184	156.498	17.389	-106.09
0.2951	42.080	17.615	109.839	0	-119.93
0.2956	41.970	17.615	109.839	0	-121.34
0.2962	41.860	17.615	109.839	0	-120.17
0.2967	41.750	17.615	109.839	0	-121.48
0.2973	41.640	17.615	109.839	0	-122.02
0.2978	41.531	17.615	109.839	0	-121.33
0.2984	41.421	17.615	109.839	0	-124.14
0.2989	41.311	17.615	109.839	0	-122.23
0.2995	41.201	17.615	109.839	0	-121.68
0.2968	11.773	4.969	30.801	3.422	-17.78
0.2972	11.743	4.965	30.801	3.422	-15.95
0.2976	11.712	4.962	30.801	3.422	-16.25
0.2980	11.681	4.959	30.801	3.422	-16.30
0.2984	11.650	4.955	30.801	3.422	-16.63
0.2988	11.619	4.952	30.801	3.422	-17.82
0.2992	11.589	4.948	30.801	3.422	-17.56
0.2996	11.558	4.945	30.801	3.422	-15.65
0.2944	11.986	5.001	30.801	3.422	-18.76
0.2948	11.955	4.998	30.801	3.422	-18.70
0.2952	11.924	4.994	30.801	3.422	-19.01
0.2960	11.863	4.987	30.801	3.422	-19.63
0.2964	11.832	4.984	30.801	3.422	-21.90
0.2968	11.801	4.981	30.801	3.422	-19.98

Continued on next page

Table S10 – continued from previous page

$x_{2,c}$	$n_{1,c}$ mmol	$n_{2,c}$ mmol	$n_{1,s}$ μmol	$n_{2,s}$ μmol	Q mJ
0.2972	11.770	4.977	30.801	3.422	-19.54
0.2976	11.739	4.974	30.801	3.422	-15.24
0.2984	11.678	4.967	30.801	3.422	-23.12
0.2988	11.647	4.963	30.801	3.422	-19.31
0.2992	11.616	4.960	30.801	3.422	-21.94
0.2996	11.585	4.957	30.801	3.422	-22.06
0.2983	43.250	18.384	142.962	35.749	-23.69
0.2986	43.107	18.348	142.962	35.749	-24.00
0.2988	42.985	18.317	122.392	30.606	-20.64
0.2991	42.862	18.287	122.392	30.606	-20.49
0.2993	42.760	18.261	101.803	25.457	-17.23
0.2995	42.659	18.236	101.803	25.457	-17.28
0.2996	42.577	18.216	81.766	20.446	-13.73
0.2998	42.495	18.195	81.766	20.446	-14.01
0.2999	42.434	18.180	61.196	15.303	-10.44
0.2983	43.253	18.385	142.962	35.749	-23.23
0.2986	43.110	18.350	142.962	35.749	-23.72
0.2988	42.988	18.319	122.392	30.606	-20.05
0.2991	42.866	18.288	122.392	30.606	-19.99
0.2993	42.764	18.263	101.803	25.457	-16.71
0.2995	42.662	18.237	101.803	25.457	-17.24
0.2996	42.580	18.217	81.766	20.446	-13.57
0.2998	42.498	18.196	81.766	20.446	-12.82
0.2999	42.437	18.181	61.196	15.303	-11.19

Table S11 Isothermal titration calorimetry data for ethylene glycol (1) + choline chloride (2) at 298.15 K. Where n_i are the number of moles of i in the cell (subscript c) or syringe (subscript s), and Q is the heat flow integral for each injection.

$x_{2,c}$	$n_{1,c}$ mmol	$n_{2,c}$ mmol	$n_{1,s}$ μmol	$n_{2,s}$ μmol	Q mJ
0.0034	12.605	0.043	57.205	14.309	14.91
0.0045	12.662	0.057	57.205	14.309	17.51
0.0056	12.719	0.072	57.205	14.309	17.42
0.0383	11.474	0.457	57.205	14.309	17.07
0.0392	11.532	0.471	57.205	14.309	17.01
0.0402	11.589	0.485	57.205	14.309	16.86
0.0411	11.646	0.500	57.205	14.309	16.87
0.0421	11.703	0.514	57.205	14.309	16.45
0.0430	11.760	0.528	57.205	14.309	16.54
0.0439	11.818	0.542	57.205	14.309	16.24
0.0383	11.423	0.455	57.205	14.309	17.19
0.0392	11.480	0.469	57.205	14.309	17.04
0.0402	11.537	0.483	57.205	14.309	17.03
0.0411	11.594	0.498	57.205	14.309	16.90
0.0421	11.651	0.512	57.205	14.309	16.59
0.0430	11.709	0.526	57.205	14.309	16.20
0.0439	11.766	0.540	57.205	14.309	16.32
0.0959	10.360	1.099	88.972	0	16.83
0.0967	10.271	1.099	88.972	0	16.21
0.0974	10.182	1.099	88.972	0	14.91
0.0982	10.093	1.099	88.972	0	15.38
0.0984	41.900	4.573	71.460	0	5.39
0.0986	41.828	4.573	71.460	0	5.42
0.0987	41.757	4.573	71.460	0	5.47
0.0989	41.686	4.573	71.460	0	5.55
0.0990	41.614	4.573	71.460	0	5.42
0.0992	41.543	4.573	71.460	0	5.48
0.0993	41.471	4.573	71.460	0	5.54
0.0995	41.400	4.573	71.460	0	5.65
0.0996	41.328	4.573	71.460	0	5.61
0.1375	9.297	1.482	71.460	0	6.93
0.1384	9.226	1.482	71.460	0	6.65
0.1393	9.154	1.482	71.460	0	7.45
0.1402	9.507	1.550	178.427	0	23.10
0.1425	9.329	1.550	178.427	0	26.14
0.1449	9.150	1.550	178.427	0	26.75
0.1403	9.605	1.567	178.427	0	22.86
0.1449	9.248	1.567	356.854	0	51.81
0.1882	8.494	1.969	88.972	0	29.46
0.1898	8.405	1.969	88.972	0	30.53
0.1914	8.316	1.969	88.972	0	30.98
0.1931	8.227	1.969	88.972	0	31.30

Continued on next page

Table S11 – continued from previous page

$x_{2,c}$	$n_{1,c}$ mmol	$n_{2,c}$ mmol	$n_{1,s}$ μmol	$n_{2,s}$ μmol	Q mJ
0.1948	8.138	1.969	88.972	0	32.13
0.1965	8.049	1.969	88.972	0	32.61
0.1983	7.960	1.969	88.972	0	33.00
0.1970	33.709	8.269	71.460	0	26.77
0.1973	33.637	8.269	71.460	0	26.64
0.1976	33.566	8.269	71.460	0	27.12
0.1980	33.494	8.269	71.460	0	27.74
0.1983	33.423	8.269	71.460	0	27.58
0.1987	33.352	8.269	71.460	0	27.05
0.1990	33.280	8.269	71.460	0	27.47
0.1994	33.209	8.269	71.460	0	27.75
0.1997	33.137	8.269	71.460	0	27.50
0.2449	30.254	9.813	71.460	0	41.30
0.2454	30.183	9.813	71.460	0	41.31
0.2458	30.111	9.813	71.460	0	41.56
0.2462	30.040	9.813	71.460	0	41.99
0.2467	29.968	9.813	71.460	0	41.96
0.2471	29.897	9.813	71.460	0	42.10
0.2476	29.825	9.813	71.460	0	42.02
0.2480	29.754	9.813	71.460	0	42.35
0.2485	29.682	9.813	71.460	0	42.46
0.2489	29.611	9.813	71.460	0	42.17
0.2494	29.540	9.813	71.460	0	42.55

Table S12 Isothermal titration calorimetry data for 1,3-propanediol (1) + choline chloride (2) at 298.15 K. Where n_i are the number of moles of i in the cell (subscript c) or syringe (subscript s), and Q is the heat flow integral for each injection.

$x_{2,c}$	$n_{1,c}$ mmol	$n_{2,c}$ mmol	$n_{1,s}$ μmol	$n_{2,s}$ μmol	Q mJ
0.0005	10.111	0.005	19.270	4.763	13.27
0.0009	10.130	0.010	19.270	4.763	13.76
0.0014	10.149	0.014	19.270	4.763	13.76
0.0019	10.168	0.019	19.270	4.763	14.47
0.0023	10.188	0.024	19.270	4.763	13.95
0.0028	10.207	0.029	19.270	4.763	14.42
0.0032	10.226	0.033	19.270	4.763	14.73
0.0037	10.245	0.038	19.270	4.763	14.44
0.0042	10.265	0.043	19.270	4.763	14.69
0.0046	10.284	0.048	19.270	4.763	14.30
0.0051	10.303	0.052	19.270	4.763	14.47
0.0055	10.323	0.057	19.270	4.763	14.60
0.0060	10.342	0.062	19.270	4.763	14.68
0.0064	10.361	0.067	19.270	4.763	14.61
0.0068	10.380	0.071	19.270	4.763	14.60
0.0981	8.608	0.937	27.384	0	4.45
0.0984	8.581	0.937	27.384	0	4.33
0.0987	8.553	0.937	27.384	0	4.37
0.0990	8.526	0.937	27.384	0	4.47
0.0993	8.498	0.937	27.384	0	4.46
0.0996	8.471	0.937	27.384	0	4.52
0.0998	8.444	0.937	27.384	0	4.49
0.1478	32.351	5.610	55.141	0	19.42
0.1480	32.295	5.610	55.141	0	19.31
0.1482	32.240	5.610	55.141	0	19.26
0.1484	32.185	5.610	55.141	0	19.35
0.1487	32.130	5.610	55.141	0	19.66
0.1489	32.075	5.610	55.141	0	19.58
0.1491	32.020	5.610	55.141	0	20.03
0.1493	31.965	5.610	55.141	0	19.68
0.1495	31.909	5.610	55.141	0	19.92
0.1878	7.445	1.721	68.653	0	36.91
0.1892	7.376	1.721	68.653	0	37.40
0.1906	7.308	1.721	68.653	0	37.95
0.1921	7.239	1.721	68.653	0	38.46
0.1936	7.170	1.721	68.653	0	38.91
0.1951	7.102	1.721	68.653	0	39.60
0.1966	7.033	1.721	68.653	0	39.94

Table S13 Dissolution calorimetry data for choline chloride (ChCl) dissolved in water (H_2O) + ChCl, ethylene glycol (EG) + ChCl, and 1,3-propanediol (13PD) + ChCl mixtures at 298.15 K. Where n_i are the number of moles of i in the cell (subscript c), or cartridge (subscript cart), and Q_{sol} is the heat of dissolution. We also list the heat of mixing (Q) calculated from Q_{sol} and ChCl fusion properties using the four discussed values for $\Delta_{\text{fus}}C_{p,\text{ChCl}}$ (ΔC_p).

component	x_2	$n_{1,c}$ mmol	$n_{2,c}$ mmol	$n_{2,\text{cart}}$ μmol	$\Delta C_p \rightarrow$		0	9.7	20.3	30.9
					1	2	Q_{sol} mJ	Q mJ	Q mJ	Q mJ
H ₂ O	ChCl	0.00000	1387.887	0.000	724.201	9299.17	-12499.28	-8984.85	-5999.83	-3014.81
		0.29963	353.786	151.355	725.677	10869.65	-10973.23	-7451.63	-4460.53	-1469.43
EG	ChCl	0.00000	266.269	0.000	76.207	1518.14	-775.69	-405.87	-91.76	222.35
		0.00000	265.994	0.000	65.965	1333.99	-651.55	-331.43	-59.54	212.36
		0.00000	266.025	0.000	65.678	1356.93	-619.99	-301.26	-30.55	240.17
		0.00022	266.133	0.060	122.475	2542.80	-1143.71	-549.35	-44.53	460.29
		0.00025	266.025	0.066	69.546	1410.53	-682.80	-345.31	-58.65	228.00
		0.00025	265.994	0.066	62.169	1276.00	-595.28	-293.58	-37.34	218.91
		0.00029	266.269	0.076	70.405	1380.59	-738.61	-396.95	-106.75	183.45
		0.00055	266.269	0.147	69.474	1414.82	-676.36	-339.21	-52.85	233.51
		0.10000	212.627	23.626	158.287	3214.40	-1550.03	-781.89	-129.46	522.97
		0.19977	170.398	42.537	66.609	1320.09	-684.85	-361.61	-87.06	187.50
		0.20000	169.816	42.455	104.283	2063.00	-1075.92	-569.85	-140.02	289.82
		0.20002	170.398	42.604	68.042	1373.84	-674.22	-344.02	-63.57	216.89
13PD	ChCl	0.00000	216.777	0.000	110.586	2853.30	-475.33	61.32	517.14	972.95
		0.00051	216.777	0.111	53.717	1226.90	-389.99	-129.31	92.10	313.52

Table S14 Redlich–Kister polynomial fitting parameters for the normalised molar excess Gibbs energy (G^E/RT) of H_2O + choline chloride (ChCl), ethylene glycol (EG) + ChCl, and 1,3-propanediol (13PD) + ChCl mixtures at 298.15 K. The parameters were obtained by fitting the normalised partial molar excess Gibbs energies (G_i^E/RT) listed in Table S5–S9.

component		$\Delta_{\text{fus}}C_{p,\text{ChCl}}$ $\text{J}\cdot\text{mol}^{-1}\cdot\text{K}^{-1}$	p_0	p_1
1	2			
13PD	ChCl	0.0	-5.514	0.884
		9.7	-4.379	0.996
		20.3	-3.231	0.947
		30.9	-2.083	0.898
EG	ChCl	0.0	-6.609	-0.597
		9.7	-5.264	-0.336
		20.3	-3.951	-0.278
		30.9	-2.638	-0.227
H ₂ O	ChCl	0.0	-9.275	-3.251
		9.7	-7.548	-2.806
		20.3	-5.897	-2.606
		30.9	-4.246	-2.407

Table S15 Redlich–Kister polynomial fitting parameters for the normalised molar excess enthalpy (H^E/RT) of $\text{H}_2\text{O} + \text{choline chloride} (\text{ChCl})$, ethylene glycol (EG) + ChCl, and 1,3-propanediol (13PD) + ChCl mixtures at 298.15 K. The parameters were obtained by fitting $Q/RT \sum \Delta n_i$, as described in section SI–1.3. Values of Q are listed in Table S10–S13.

component		$\Delta_{\text{fus}} C_{p,\text{ChCl}}$	p_0	p_1	p_2
1	2	$\text{J}\cdot\text{mol}^{-1}\cdot\text{K}^{-1}$			
13PD	ChCl	20.3	-15.932	14.187	-4.057 ^a
		0.0	-7.161	5.427	
		9.7	-3.891	4.113	
		20.3	-1.114	2.998	
		30.9	1.664	1.882	
EG	ChCl	20.3	-24.059	20.981	-8.013 ^a
		0.0	-7.669	4.237	
		9.7	-4.321	2.788	
		20.3	-1.477	1.557	
		30.9	1.367	0.326	
H ₂ O	ChCl	20.3	56.775	-48.442	20.088 ^a
		0.0	-11.925	4.913	
		9.7	-8.361	3.281	
		20.3	-5.333	1.895	
		30.9	-2.305	0.509	

^a Fit only to H_1^E/RT

Table S16 Positions of first maximum and minimum of radial distribution functions between the H atom of the HBD.

x_{ChCl}	$r_{\text{max}} / \text{\AA}$	$r_{\text{min}} / \text{\AA}$
Ethylene glycol		
$\text{H}_{\text{EG}} \cdots \text{O}_{\text{EG}}$		
0.0	1.983	2.583
0.1	1.983	2.550
0.3	1.983	2.417
$\text{H}_{\text{EG}} \cdots \text{Cl}$		
0.1	2.150	3.183
0.3	2.116	2.917
Water		
$\text{H}_{\text{H}_2\text{O}} \cdots \text{O}_{\text{H}_2\text{O}}$		
0.0	1.850	2.450
0.1	1.817	2.317
0.3	1.783	2.250
$\text{H}_{\text{H}_2\text{O}} \cdots \text{O}_{\text{Ch}}$		
0.1	1.450	2.283
0.3	1.450	2.283
$\text{H}_{\text{H}_2\text{O}} \cdots \text{Cl}$		
0.1	2.017	2.850
0.3	2.050	2.910

Table S17 Positions of first maximum and minimum of radial distribution functions between the center of mass of Ch and Cl and corresponding coordination number. In the right-most column the percentage deviation from the expected value considering the change in salt concentration.

x_{ChCl}		$r_{\max} / \text{\AA}$	$r_{\min} / \text{\AA}$	n_{coord}	$\delta / \%$
Ethylene glycol					
$\text{Ch}_{\text{COM}} \cdots \text{Cl}_{\text{COM}}$					
0.1		5.054	7.296	1.36	
0.3		5.054	6.613	3.26	-3
Water					
$\text{Ch}_{\text{COM}} \cdots \text{Cl}_{\text{COM}}$					
0.1		4.891	6.874	3.44	
0.3		4.859	6.453	5.11	-12

References

- [1] D. Bohne, S. Fischer, E. Obermeier, *Berichte der Bunsengesellschaft für Phys. Chemie* **1984**, *88*, 739–742.
- [2] J. Dean, *Mater. Manuf. Process.* **1990**, *5*, 687–688.
- [3] S. M. Vilas-Boas, D. O. Abrançhes, E. A. Crespo, O. Ferreira, J. A. P. Coutinho, S. P. Pinho, *J. Mol. Liq.* **2020**, *300*, 112281.
- [4] R. B. Leron, A. N. Soriano, M.-H. Li, *J. Taiwan Inst. Chem. Eng.* **2012**, *43*, 551–557.
- [5] K. Shahbaz, F. S. Mjalli, M. Hashim, I. AlNashef, *Thermochim. Acta* **2011**, *515*, 67–72.
- [6] K. Shahbaz, S. Baroutian, F. Mjalli, M. Hashim, I. AlNashef, *Thermochim. Acta* **2012**, *527*, 59–66.
- [7] A. Yadav, J. R. Kar, M. Verma, S. Naqvi, S. Pandey, *Thermochim. Acta* **2015**, *600*, 95–101.
- [8] Y. Zhang, D. Poe, L. Heroux, H. Squire, B. W. Doherty, Z. Long, M. Dadmun, B. Gurkan, M. E. Tuckerman, E. J. Maginn, *J. Phys. Chem. B* **2020**, *124*, 5251–5264.
- [9] Y. Zhang, H. Squire, B. Gurkan, E. J. Maginn, *J. Chem. Eng. Data* **2022**, *67*, 1864–1871.
- [10] A. van den Bruinhorst, J. Avila, M. Rosenthal, A. Pellegrino, M. Burghammer, M. Costa Gomes, *Nat. Commun.* **2023**, *14*, 6684.
- [11] A. I. M. C. Lobo Ferreira, S. M. Vilas-Boas, R. M. A. Silva, M. A. R. Martins, D. O. Abrançhes, P. C. R. Soares-Santos, F. A. Almeida Paz, O. Ferreira, S. P. Pinho, L. M. N. B. F. Santos, J. A. P. Coutinho, *Phys. Chem. Chem. Phys.* **2022**, *24*, 14886–14897.
- [12] I. C. M. Vaz, A. I. M. C. Lobo Ferreira, G. M. C. Silva, P. Morgado, D. O. Abrançhes, M. Bastos, L. M. N. B. F. Santos, E. J. M. Filipe, J. A. P. Coutinho, *Phys. Chem. Chem. Phys.* **2023**, *25*, 11227–11236.
- [13] R. Feistel, D. G. Wright, K. Miyagawa, A. H. Harvey, J. Hruby, D. R. Jackett, T. J. McDougall, W. Wagner, *Ocean Sci.* **2008**, *4*, 275–291.
- [14] E. S. Domalski, E. D. Hearing, *J. Phys. Chem. Ref. Data* **1996**, *25*, 1–525.
- [15] G. S. Parks, K. K. Kelley, *J. Am. Chem. Soc.* **1925**, *47*, 2089–2097.
- [16] Z. Nan, B. Liu, Z. Tan, *J. Chem. Thermodyn.* **2002**, *34*, 915–926.
- [17] J. B. Macaskill, M. S. Mohan, R. G. Bates, *Anal. Chem.* **1977**, *49*, 209–212.
- [18] I. Khan, K. A. Kurnia, T. E. Sintra, J. A. Saraiva, S. P. Pinho, J. A. P. Coutinho, *Fluid Phase Equilib.* **2014**, *361*, 16–22.
- [19] H. Zhang, M. L. Ferrer, M. J. Roldán-Ruiz, R. J. Jiménez-Riobóo, M. C. Gutiérrez, F. del Monte, *J. Phys. Chem. B* **2020**, *124*, 4002–4009.
- [20] E. Mangiacapre, F. Castiglione, M. D'Aristotile, V. Di Lisio, A. Triolo, O. Russina, *J. Mol. Liq.* **2023**, *383*, 122120.
- [21] V. Agieienko, R. Buchner, *Phys. Chem. Chem. Phys.* **2022**, *24*, 5265–5268.